Aggregating rods: applications to angiogenesis

Author:
Kleopatra Pirpinia

Supervisors:
Prof. dr. Odo Diekmann
Utrecht University
Dr. Roeland Merks
CWI
Second reader:
Dr. Paul A. Zegeling

Master Thesis

December 9, 2013

Universiteit Utrecht

CWI
Centrum Wiskunde & Informatica

Preface

This thesis is the result of nine months of work in the Biomodeling and Biosystems Analysis group at the Center for Mathematics and Computer Science (CWI). First of all, I would like to thank my daily supervisor Roeland Merks for his guidance, which was fundamental for the completion of this thesis, and his continuous encouragement, which has been equally important. I would also like to thank my supervisor and tutor in Utrecht Odo Diekmann, for his feedback on the thesis, and his help during the two years of this master.

I would like to dedicate this thesis to my parents, who have helped me in every possible way study what I have always loved, and to my friends, who have supported me a lot through the years. Lastly, I would dedicate it to Davide, who has been always there, in the good moments and the bad ones, in this journey we started together.

Contents

Chapter 1

Introduction

1.1 Biological background

Angiogenesis is the physiological process through which there is formation of new blood vessels, from sprouting or splitting of pre-existing ones [1]. It is fundamental in normal physiology during wound healing and new tissue formation, as almost all tissues develop vascular networks that provide the cells with nutrients and oxygen. It is regulated by chemicals, some of which stimulate blood vessel formation (and are called angiogenic growth factors) and others inhibit it (angiogenesis inhibitors) [2]. Once formed, the vascular network is a stable system that regenerates slowly.

Pathological angiogenesis though, which is the abnormal unregulated by the body proliferation of blood vessels, is implicated in over 20 diseases, including cancer, where it occurs during tumor growth as well as metastasis . It is actually vital to tumor growth since it feeds and sustains them, and for this reason angiogenic growth factors are targeted, in order to 'starve' off the cancerous cells by preventing creation of new blood vessels [3]. During metastasis, it is essential because it helps the cancerous cells migrate to distant organs via blood.

The angiogenic process goes briefly as follows. Initially, there is secretion of angiogenic growth factors by the diseased (tumor) or injured tissue [4], which diffuse into the already existing nearby blood vessels. These growth factors then bind to certain receptors, which are located on the cells that line up the blood vessels, called endothelial cells (ECs). Then the endothelial cells become activated, and produce enzymes that create 'holes' into the cover that surrounds the blood vessels (the *basement membrane*). Through these 'holes' the ECs start proliferating and migrating towards the tissue. Special adhesion molecules help the forming tip of the new blood vessel sprout forward, and other enzymes dissolve the tissue in order to accomodate it [1]. Gradually the ECs proceed in forming blood vessel tubes, which then connect to form loops through which blood can circulate.

It becomes clear that angiogenesis is fundamental in many processes, in normal

physiology as well as in disease, therefore the understanding of the underlying mechanisms that drive it is of great importance. What we are interested in is the process in the initial stages, where there is collective motion of endothelial cells that adhere to each other in order to form the vascular network. We would like to comprehend which intrinsic mechanisms strictly associated to the cells contribute to the formation of the network, and to which extent. There are also other central questions that need to be answered such as: is self-organisation and short range interaction among the cells sufficient for the creation of such patterns, or are external mechanisms (such as chemotaxis) necessary?

In order to study the different aspects of angiogenesis, several mathematical and computational models have been employed, a brief overview of which will be discussed in the following section. Since we focus on the initial stages where collective motion is the main element, more general models that give insight into this mechanism in particular will be presented.

1.2 Mathematical modeling of angiogenesis

First, acknowledging that self-organization is a fundamental factor in angiogenesis, we will view it in a general framework, since it is a process that occurs in a big variety of physical, chemical, social and biological systems. It can be defined as a process where an initially disordered system exhibits some form of ordering through solely local interactions among its components. In chemistry self-organising phenomena can be observed in liquid and colloidal crystals as well as in various reaction-diffusion systems, whereas in biology various processes can be characterized as such: pattern formation and morphogenesis (the growing and development of an organism), the origin of life itself from self-organising chemical systems, and flocking behaviour (observed in the motion of birds and fish).

Mathematical models have been very useful in providing insight into these systems. One of the most famous models that study collective behaviour is the Viscek model [5], where the concept of self-propelled particles was first introduced. Self-propelled (or self-driven) particles act as autonomous objects that follow simple rules that govern their behaviour. In the Viscek model, the particles are characterized by their position, their velocity, which remains constant at all times, and their velocity angle, which expresses their direction of motion. The main idea of the model is that every particle follows the motion of its neighbors, by moving in the average direction of its neighbors. This is not absolute though, since every particle can respond in every time step to a random perturbation that can change its direction, and it is called *noise*. These perturbations can be *extrinsic*, which means they can come from the environment (for example, they can be seen as 'mistakes' in the interaction among the particles which result in a wrong direction) or *intrinsic*, which means that they come from the particle itself; it decides to move randomly towards a different direction. Vicsek and collaborators showed that with the presence of intrinsic noise that increases, an initially ordered system where all particles point towards the same direction

undergoes a transition to a disordered state of particles moving in random uncorrelated directions. They also find that for a certain range of particle density and noise parameter, collective motion can occur.

Another interesting model is the one proposed by Grégoire, Chaté, and Tu [6]. Starting from the model described by Vicsek, they formulate a minimal stochastic model in which they show that there can be cohesive motion even if the particles move in a very noisy manner. They keep the velocity angle which indicates the direction of the particles as well as their tendency to align with each other, without eliminating the perturbations. The interesting new element is the addition of a physical aspect of the particles, by incorporating short range interaction through forces. Depending on the distance among the particles, these forces become attracting or repulsive. They extend the noise term to include a noise parameter related to the forces. They repeat the experiments studying the effect of the noise parameter and the particle density, detecting phase transitions from gas-like to liquid-like phases, which are quantified with the use of several order parameters. They as well detect cohesive motion for certain domains of the two parameters.

Returning to the context of blood vessel growth and network formation, there have been different approaches for the modeling of angiogenesis and vasculogenesis (which is the process of formation of blood vessels *de novo*); continuous models, computational/numerical models, hybrid approaches, mechanics-based approaches, each one with its strengths and weaknesses. In most continuous models, the main assumption is that the main mechanism that drives angiogenesis is the interaction between the cells and the extracellular matrix, the tissue that provides structural stability and contains the surface where the endothelial cells move. Such a continuous, mechanical model is the one by Manoussaki et al. [7], where it is assumed that the cells apply stress on the surface of the matrix, which in turn creates traction, and helps them move. On the other hand, the matrix is modelled as a viscous, deformable material. The cells are described in terms of densities $n(x,t)$ (number of cells per unit area), as well as the matrix with $(\rho(x,t))$ the matrix density, which corresponds to thickness. The density changes are then quantified by using conservation laws. It is concluded that cell traction is a critical factor for the formation of networks, as well as the degree of stiffness of the extracellular matrix. In another continuous mathematical model, the presence of a chemoattractant was assumed; a chemoattractant is a substance that induces movement of the cells in the direction of its highest concentration, in a phenomenon that is called chemotaxis. Assuming moreover persistence in motion of the cells, the importance of the chemoattractant's presence was concluded [8] [9]. The system was described with differential equations and a mass conservation equation in terms of cell densities ρ_c, their velocity v_c and the concentration of the chemoattractant c.

Although continuous models are able to describe the angiogenic process quite accurately, assuming presence of chemotaxis, forces between the cells and the substratum as well as persistent motion, the interactions at the cellular level are hard to capture. Cell-based models are more adequate in order to capture

the effect of biophysical properties of individual cells on collective behaviour. A widely used simulation technique is the Cellular Potts Model, which is a modeling framework which follows an energy minimization philosophy [10] and will be discussed in more detail as it will form the starting point for our approach.

1.2.1 The Cellular Potts Model

The CPM proposed by Glazier and Graner in 1992, is a lattice-based Monte-Carlo modeling framework which is used to simulate collective cell behaviour. A two-dimensional lattice is used. Every site x of a lattice is assigned a spin $\sigma(x)$ which is an integer number. Connected sites (neighboring sites) which have identical spin represent a discrete object, of a certain type $\tau(\sigma)$.

In the framework of vasculogenesis / angiogenesis, the two different types can be a cell, and the matrix (the surrounding). The system is described by its effective energy H, or alternatively Hamiltonian. Each time, a lattice site tries to copy its spin to one of its neighboring sites (randomly selected), and the attempt is always accepted if there is a decrease in the total energy, otherwise it is accepted with a certain probability which follows the Boltzmann distribution. H is a functional that represents the whole energy of the system, and consists of several terms which express cell properties, such as shape and size, true energies such as cell-cell adhesion, and terms that describe chemical effects such as chemotaxis. If we have $\Delta H = H_{after} - H_{before}$:

$$P(\Delta H) = \begin{cases} 1, & \text{if } \Delta H \leq 0 \\ e^{-\frac{\Delta H}{T}}, & \text{if } \Delta H > 0. \end{cases}$$

For a particular CPM model of vasculogenesis where also presence of chemotaxis was assumed [11], we have that

$$H = H_{adhesion} + H_{area} + H_{chemical}.$$

The first term is

$$H_{adhesion} = \sum_{i,j} J_{\tau((\sigma(i)),\tau(\sigma(j))}(1 - \delta_{(\sigma(i),\sigma(j))})$$

where i, j are neighboring lattice sites, and τ denotes the type of objects that interact; in this specific case, the different types can either be a cell, or the extracellular matrix. It is clear that when two neighboring cites have the same spin ($\sigma(i) = \sigma(j)$) thus they belong to the same cell, the energy that adhesion costs is 0. The second term is a geometrical constraint, and penalizes the attempt of a cell to increase its area, because of the assumptions that the cells don't grow or divide. Thus

$$H_{area} = \sum_{i} \lambda_{area} \left[V(\sigma(i)) - V_t(\sigma(i))\right]^2,$$

where V denotes the actual surface area of the cell and V_t the target area.

The last term describes the biased walk of the cells up towards the gradient of the chemoattracting substance, and is implemented in a way that ensures that chemotactic interactions occur only between the cells and the matrix.

A schematic representation of the CPM can be seen in Figure 1.1.

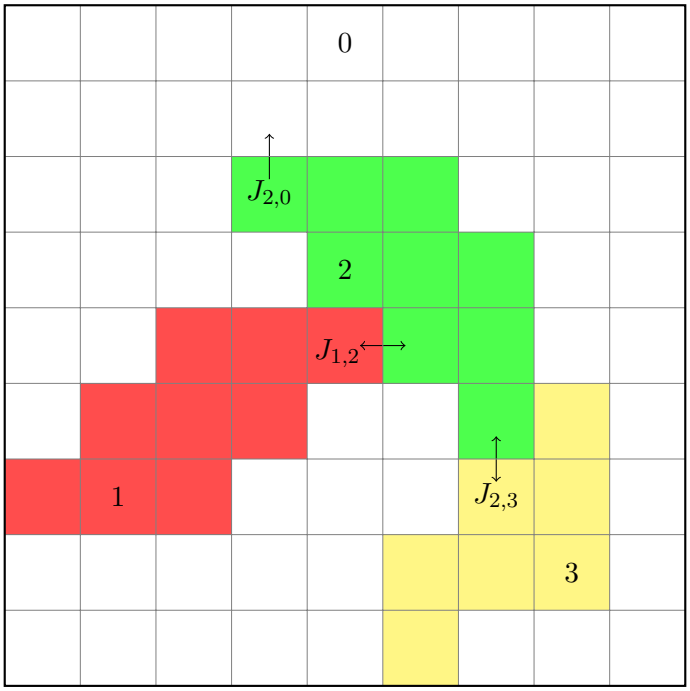

Figure 1.1: Schematic representation of the Cellular Potts Model and the energy interactions between cells of spin 1, 2, 3 and their surrounding (which is of different type and spin 0).

1.2.2 A computational model for angiogenesis

Elongated shape proves to be essential for the *in silico* creation of network like patterns in vasculogenesis [12]. In the Cellular Potts modelling framework, M. Palm and R.Merks proposed a computational, lattice-based Monte Carlo model [13] for the movement of elongated cells, which will be of particular interest to us. The only assumptions that are made are that cells move and rotate freely, interacting only via adhesion. In a subset of simulations, also the presence of chemotaxis is assumed, described macroscopically with a diffusion equation. There are also area and volume constraints, in order to avoid situations where cells slide over each other or divide.

The numerical simulations for round cells show formation of round clusters of cells, whereas when the cells have elongated shape there is emergence of network-

like structures; these stabilize and turn into a clear network only when chemotaxis is present. In the absence of chemotaxis, cells continue to align to each other with increasing difficulty as the cluster becomes bigger, gradually creating network-like structures that move very slowly. Consequently, they enter a state of 'arrested dynamics', where the system seems to evolve towards an equilibrium, but does not reach it. All three cases can be seen in Figure 1.2.

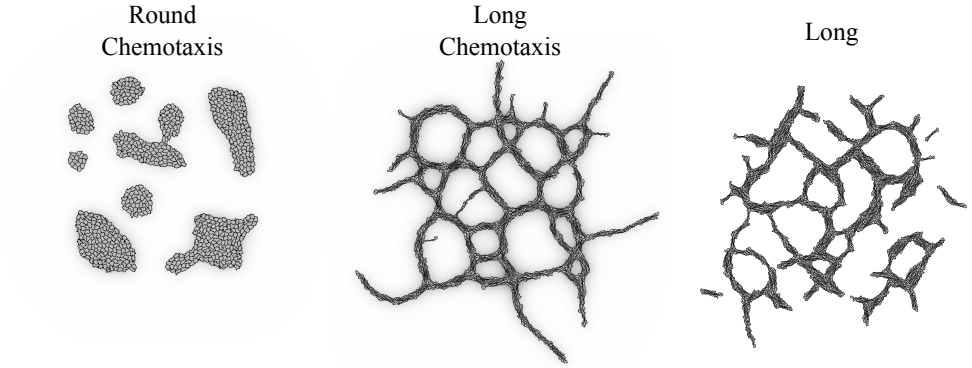

Figure 1.2: Results for round and chemotacting, long and chemotacting, and long and non-chemotacting cells (Image courtesy of Palm and al. [13].
)

While the CPM is able to produce interesting patterns, by its very construction is a very difficult starting point for deeper study. Since we want to focus also on the type of motion of the cells, a continuous space model would be more adapted and accurate. Moreover, the cell is not a single object but a collection of pixels, to which these biophysical properties are assigned, thus it is difficult to analyse. For this reason, we would like to propose a model which stays close to the nature of the CPM and reproduces the above pattern, but might be also a step towards a more analytical approach. The aim is to formulate a model that will be the first step for a rigorous mathematical analysis, which in its turn would give more insight into the long term behavior of this system and the phenomenon of arrested dynamics.

In order to formulate this model, we thought of two approaches: a continuous approach which will be described briefly below in section 1.3, and a discrete particle-based approach which will be described in more detail in Section 1.4. We will then proceed in Section 4.1 to briefly describe a model of aggregation phenomena which presents phenomenological similarities; thus it seems an interesting direction. Finally in Section 1.5 we will discuss some terms that will be used in our methods and are taken from the theory of liquid crystals.

1.3 A partial differential equations approach

As mentioned before, formulation of continuum models is very useful when we want to analyze the theoretical basis of a mechanism - these models are usually

sets of partial differential equations which describe the dynamics of the system in question. One example of such a model is presented in the paper by R. Hawkins, S. Tindemans and B. Mulder[14][15], on the orientational ordering of the microtubules. Microtubules are self-propelled protein aggregates which align with each other in order to form the cortical array, a major component of the cytoskeleton in eukaryotic organisms. They are fixed in space, but nonetheless they seem to move across the plane, due to *treadmilling*, the process of simultaneous polymerization of one part and depolymerization of the other part.

The microtubules are modelled as rigid elongated rods, with rotational and translational degrees of freedom. Each one has a 'plus' end that is either growing or shrinking. This segment at the end of the microtubule is called 'active' and is the one taken into consideration. The segment can switch stochastically from growing to shrinking (in a phenomenon called catastrophe) or from shrinking to growing (a so-called rescue). New microtubules can also be created (nucleation). The microtubules can also rotate randomly; their orientation is described by tθ, which is the angle of the rod with an arbitrary axis. There is no interaction between them apart from the collision events, the outcomes of which are functions of their angle of collision $|\theta - \theta'|$. Depending on the angle, the result of the collision can either be a catastrophe, a rescue, or a zippering event: in that case, the active segment of the one microtubule bends to the direction of the other one, becoming inactive, and a new segment is created alongside the other microtubule. The smaller the angle is, the higher the probability of the zippering event. The inverse can also occur; if the active segment shrinks to zero length, then the connected segment that was previously inactive can be reactivated towards another direction. It is necessary to keep track of the position of the active segments as follows: a segment i which is connected directly to its nucleation site, has $i = 1$. This number increases after every zippering event, when a new active segment is created. The dynamics of movement are described by differential equations, in terms of changes in the cell densities.

The fundamental variables of the system are the areal number densities $m_i^\sigma(l, \theta, t)$ of segments i in state $\sigma \in \{0, -, +\}$ with i having length l and orientation θ at time t. The master equations for these densities can be written as follows:

$$\partial_t m_i^+(l, \theta, t) = \Phi_{growth} + \Phi_{rescue} - \Phi_{spont.cat.} - \Phi_{induced\ cat} - \Phi_{zipper}$$

$$\partial_t m_i^-(l, \theta, t) = \Phi_{shrinkage} - \Phi_{rescue} + \Phi_{spont.cat.} - \Phi_{induced\ cat} + \Phi_{reactivation}$$

$$\partial_t m_i^0(l, \theta, t) = \Phi_{zipper} - \Phi_{reactivation}.$$

These equations must be supplemented by the appropriate boundary conditions. For the initial segments ($i = 1$) this corresponds to the creation of new microtubules. For the rest of the segments ($i > 1$) it corresponds to the creation of

new segments as the result of a zippering event. Therefore, the boundary conditions are different for every value of i. This leads to an infinite set of coupled equations, three for every value of i.

The above description is the starting point of the authors, which show that the system in the steady state can be reduced in a finite set of equations.

The model described briefly above presents an approach which could be very useful for our purpose, since it contains many similar elements, such as the representation of the microtubules as rigid elongated objects, that diffuse, with out any interaction mechanisms. Moreover, even after a zippering event which causes them to move together, they are not considered as one bundle - they diffuse and rotate independently which is something we would like to reproduce. It is also a continuous model, and the zippering event that is presented is very similar to the alignment of two elongated cells that collide with a small angle.

Although the continuum approach has these advantages, its main disadvantage is the fact that the identity of the individuals is compromised, which makes it more appropriate for describing large and dense populations. Since we are interested in which properties and specific interactions among the cells have the biggest effect on their collective motion, we oriented ourselves towards an individual based approach, where each cell is considered a discrete particle subject to rules of movement. This is still a different approach from the Cellular Potts, where each cell is a set of discrete objects.

1.4 A particle-based approach

The approach we discuss here is based on the work by A.Stevens and H.Othmer[16]. The authors wish to understand biological systems where the movement of the organism is regulated by the presence of a substance which acts as a signal. This substance is usually diffusible, but in certain systems this is not true; there is the possibility that this regulating substance modifies the environment in a very local manner, which leads to indirect or short range interactions among the organisms of the system. Whereas the first case of the diffusible regulator can be easily modelled using diffusion equations, the second case is best modelled as a random walk.

The authors take as an example the motion of myxobacteria, bacteria which live in the soil and feed on organic substances. Myxobacteria move by gliding and interact non directly, by releasing a non-diffusible substance called slime and adapt their movement following its trail. They eventually aggregate in order to form fruiting bodies. Their motion is modelled in the framework of stochastic cellular automata, which we explain below.

1.4.1 Stochastic cellular automata

A (deterministic) cellular automaton is a discrete model which can be very useful in simulating several stochastic processes that occur in nature. It can be characterised as a discrete dynamical system of interacting objects. It can be simply described as a grid of cells (objects), and each one can be in a finite number of states. Each cell is initially in a certain state, which is updated based on a fixed rule (a mathematical function), which is dependent on the current state of the cell as well as the states of its neighborhood. The rule is the same for all cells, and the updates occur simultaneously for all.

In order to take into account random events, a variant of the cellular automaton was formulated. It is called a *stochastic (or probabilistic) cellular automaton* (PCA), where all the cells evolve synchronously and the rule according to which they update their state follows a probability distribution, which depends only on a finite neighborhood of the cell. The behavior that is observed based on such simple rules can be surprisingly complex. Self-organization is known to be exhibited bu such automata. A PCA is a mathematical object; it can be characterized in the framework of stochastic processes as a discrete-time Markov process which desribes a random dynamical system for locally interacting particles.

One sees easily that the Cellular Potts Model described in Section 1.2.1 can be considered a stochastic cellular automaton.

Returning to the system of Othmer and Stevens, this system is modeled with a stochastic automaton model, where bacteria are represented as elongated particles on a lattice, with a realistic length-to-width relationship. The particles undergo a reinforced random walk - reinforced because additional weights are added to the points on the lattice that are visited more often, thus increasing the probability of being visited again. The weights represent the quantity of the regulator substance, which is the slime. The automaton is stochastic because also noise is incorporated in the transition probability from one state to the other.

The numerical simulations with this model show that some pre-aggregation patterns occur, which are unstable and soon dissolve. Therefore as a next step, the authors incorporate chemotaxis in a set of simulations, which is observed to stabilize the aggregation pattern.

The authors then model the process as a Markov chain, and derive equations for continuous approximations of a continuous time, discrete-space random walk. They describe and analyse using differential equations the variety of patterns that emerge as a result of the interplay among chemotaxis, the production of the modulator substance (which in this case is the slime) and the bacteria's response to them.

In our opinion the methods of this approach are very suitable for the problem we want to study. First of all, the questions that are to be answered are the same: are strictly local interactions sufficient for formation of aggregation patterns?

Most importantly, the framework of cellular automata is closely connected to

the Cellular Potts model, and as described above it can provide a way for the analytical treatment of the system. We would like to follow a similar approach, by modeling our system as a random walk initially, and then be able to study the continuum limit of this walk.

1.5 Liquid crystals

Lastly, we will discuss some concepts taken from the theory of soft matter and liquid crystals. Liquid crystal materials are characterized by a rigid long axis and a rod-like molecular structure. They are a useful analogue for the phenomenology we try to reproduce, as the shape and structure of an endothelial cell is very similar (rod-like and rigid).

Whereas molecules of an isotropic fluid have no intrinsic order, liquids in the crystalline phase display orientational ordering by tending to point towards a preferred orientation, the director. When instead they are in a solid phase they have no translational freedom. Therefore a liquid crystal is defined as a substance which is not ordered as a solid but has some degree of alignment. The phenomenology of these kinds of systems resembles the one observed by the Cellular Potts model simulations where the cells exhibit a liquid crystalline phase of 'arrested dynamics'. For this reason we believe that some concepts would be very useful for our approach, and will be explained below.

In order to quantify the degree of ordering and detect the transition of the system from one state to the other, a physical quantity called the orientational order parameter S is used. S is zero in an isotropic fluid and 1 for a perfectly aligned system. In the general case, S is calculated as follows. Firstly, we calculate the direction tensor [17]

$$Q_{\alpha\beta} = \frac{1}{N}\sum_{j=1}^{n}\left(\frac{3}{2}u_{\hat{j}\alpha}u_{\hat{j}\beta} - \frac{1}{2}\delta_{\alpha\beta}\right)$$

where N is the number of molecules. The axes x, y and z are represented by α and β, $u_{j\alpha}$, $u_{j\beta}$ are the αth, βth Cartesian coordinates of the unit vector that indicate the orientation of molecule j, and $\delta_{\alpha\beta}$ is the Kronecker delta. Diagonalizing Q gives us three eigenvalues $\lambda_+, \lambda_0, \lambda_-$. The largest eigenvalue λ_+ is S and its corresponding eigenvector n is the nematic director. Then [18]

$$S = \frac{d\langle\cos^2\theta\rangle - 1}{d-1},$$

where d is the dimensionality of the system, and $\langle\cdot\rangle$ denotes the mean over all the orientations θ of the molecules.

More insight into the theoretical derivation of S can be found in [17].

Note that this definition of S leads to an always positive quantity even in an isotropic liquid. Moreover, in a system with no long range orientational ordering S vanishes to 0 when $N \to \infty$.

Thermotropic liquid crystals - materials the state of which changes by the temperature - display various types of alignment which will prove to be useful for the characterization of our patterns. As the temperature decreases, there is a transition from an isotropic (copmletely unordered) fluid to nematic ordering, which is characterized by a degree of alignmment, and then to a smectic phase, where the molecules remain still and ordered.

In the nematic phase, which is of greatest interest to us, the molecules have no positional order (there is no formation of layers or any other ordered structures) but they only tend to point at the same direction, along the direction vector.

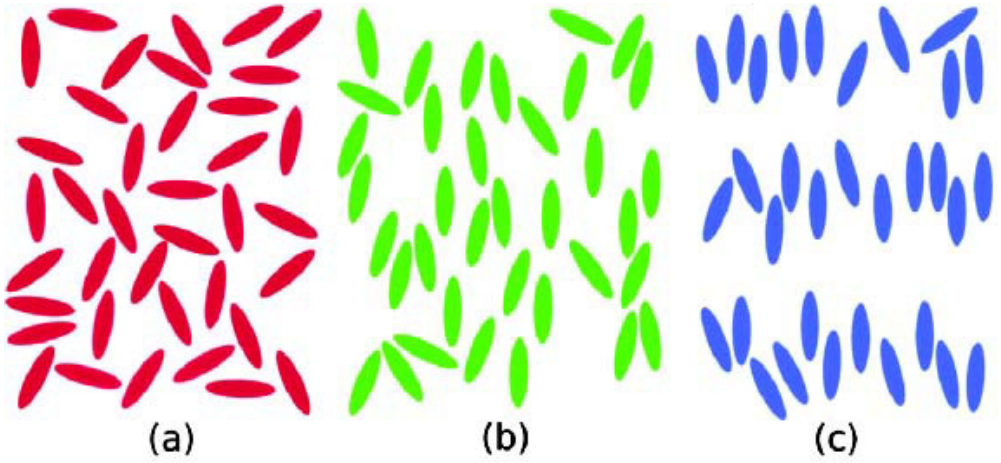

Figure 1.3: Isotropic, nematic and smectic phase of the molecules of a liquid crystal (Image courtesy of Harrison et al. [19]).

Chapter 2

Methods

As mentioned already, our aim is to find a suitable framework to model and study the motion of endothelial cells, which by moving and rotating freely proceed to aggregate and form vascular-like structures. The Cellular Potts framework produces interesting patterns, however, by the way it is constructed it cannot be a foundation for further analytical treatment of the system. Every cell in the Cellular Potts is not considered a single object, but it consists of many parts to which many constraints and properties are assigned. Therefore, it becomes difficult to say something about the cell's motion or describe it with equations. For this reason, we would like to present a different, particle-based approach which we can use in order to further study the phenomenon.

In this chapter, we first discuss our first attempt to model the system, which however was abandoned. Next, we will formulate and discuss in detail our main model, the results of which will be presented separately in Chapter 3. In both models, the mechanisms that we try to reproduce are the same. The first one is random movement, the second one is random rotation, and the third one is cell adhesion, the process by which a cell binds itself to another one, or to the environment around it. Cell adhesion is the only means of interaction among the cells in our model, and it is considered strictly local. The approach we follow in both models is closely related to the one presented in Section 1.4, where cells are particles the motion of which is governed by simple probabilistic rules. The difference with the approach presented before is that we formulate off-lattice models.

2.1 Preliminary model

Although the approach we adopt is strictly particle-based, here we model the motion of cells similarly as that of microtubules as described in Section 1.3. The cells are represented as elliptic objects, which undergo a random walk and also change their rotation randomly. We see cell adhesion as a similar mechanism to the zippering of the microtubules; when the cells are close to each other and

have a small relative angle, they form adhesive bonds, 'bind' to each other and subsequently start moving together. Each pair of cells is assigned a quantity called 'binding energy', and it represents the mechanical work that has to be done by them in order to overcome the forces that hold them together. There is the possibility that two cells detach eventually, which naturally depends on how high the binding energy of the pair is. We assume that the higher the angle of collision is, the lower their binding energy is. We proceed to formulate the above rules as follows.

2.1.1 The rules

Every cell is represented as an ellipse in the cartesian plane, and it is characterized by its long semi-axis a and its short semi-axis b. It also has an initial position expressed in cartesian coordinates (x,y) and an orientation θ, which is defined as the angle between a and the x-axis. We are in a discrete setting, therefore x, $y \in \mathbb{Z}$ as well as time $t \in \mathbb{Z}$. The orientation θ also belongs to $\mathbb{Z}$ and it is expressed in degrees, ranging from 0 to 180 because of the symmetric shape of the cells.

In every time step t, a cell updates its position by a fixed step size of 1. It can update its position in 4 possible ways; it can go up, down, left or right with equal probability $\frac{1}{4}$. More formally, if $X_t = (x_t, y_t)$ is its position at time t, we have that its position at time $t+1$ is

$$x_{t+1} = x_t + \delta x,$$
$$y_{t+1} = y_t + \delta y,$$

where $\delta x, \delta y$ can be 1 or -1. Note that there is no lattice in our model, therefore the set of possible locations that a given cell can occupy is countably infinite.

Furthermore, similarly, in every time step t it updates its orientation θ, which is completely independent from its movement, and the increment every time with which it is updated is a $\Delta\theta$, a random integer from $\{-20, \ldots, 20\}$.

After these updates, for every cell i we calculate the number its neighbours, which we consider to be the cells whose center of mass is in a circle of radius $2a$ from the center of mass of cell i. We subsequently calculate the relative angle $\theta'_{(i,j)} = |\theta_i - \theta_j|$, for every neighbour j of cell i. If $\theta'_{(i,j)} < 40$, then the two cells from the second step onwards start moving together. This is implemented by updating first the position and rotation of one of the two cells, and then by assigning the same displacements to the other one. Therefore, the procedure from the next step onwards and all the following steps, is as follows; we update the position and rotation of all cells, taking into account the pairs; Then, we assign to each cell of the pair the binding energy E which is calculated in the following way:

$$E = \frac{h}{\theta'_{(i,j)}},$$

where the parameter h is a strictly positive real number.

The probability of separation is then calculated:

$$P(E) = e^{-\frac{E}{kT}},$$

where E is the *binding energy*, T is what we call in our framework the 'cellular temperature'of the system - the degree of random motility of our cells, and k is the Boltzmann constant - the term is used since the probability defined above follows the Boltzmann distribution, widely used in statistical mechanics. In every step, before updating positions, this probability is calculated, and afterwards the positions of every cell are calculated accordingly.

2.1.2 Visualization

We tried to visualize our model using the Qt application framework, a cross-platform application framework which uses standard C++ as programming language. By using this framework we had to slightly modify our implementation, since in Qt there is the possibility to detect collisions between the objects. Nonetheless, the core of the model remains the same. The cells move and rotate freely, and as soon as they collide they start moving together.

In the Appendix, in Figure A.2, we can see the evolution of the system over time with 70 cells. For h we have used a value fixed to 2. We do not see any interesting patterns, for any value of h we tried; small groups (aggregates) of cells were formed, which later also dissolved. This implementation moreover proved to be computationally heavy (thus the low number of cells) and this was one of the reasons it was abandoned, since we could not also investigate the effect of cellular density on formation of these patterns. Therefore, we chose not to pursue more this approach and tried a different one instead, which is presented and discussed in detail in the following Section 2.2.

2.2 A numerical model for aggregating cells

As we said before, we want to model efficiently the motion of endothelial cells and their self assembly into vascular like structures. Also here we follow a particle-based approach, closely related to the work by A. Stevens and H. Othmer. We will first discuss the biological assumptions behind the model, then we will proceed to describe its numerical implementation, and finally we will discuss an attempt for a mathematical formulation, which could serve as a fist step for its analytical treatment. In the following chapter we will present and analyze the results we obtained.

2.2.1 Biological assumptions

The mechanisms on which we focus remain the same: random motion, random rotation and cell-cell interaction via adhesion. Clearly, the first two are easy to describe. However, cell adhesion is a different case, and in order to simulate it, we thought about the phenomenon of contact-inhibited motility. In biology, this inhibition of locomotion is observed in several types of cells. Specifically, it has been seen that cells tend to change direction in order to avoid collisions with the ones around them. Consequently, as density becomes higher, the number of possible directions a cell can take decrease. Furthermore, when two cells come into contact, their motion is paralyzed.

Based on this, we make a couple of assumptions which will help describe cell adhesion.

First of all, we assume that the motility of each cell is highly dependent on the density of the cells around it. The more cells surround it, the less likely it is to move. Consequently, when cells 'bump' into each other or come very close, they tend to stay still or sometimes stick.

Another assumption that we make is that a cell is sensitive to the direction of its neighbors, to which it tends to adjust. In the case of elongated cells, the direction is determined by the long axis of the cell and its angle with the x-axis. The more aligned cells are, i.e. the more parallel their long axes are, the less likely it is that they change their direction.

These two assumptions result in moving cells that tend to stay very close to each other as well as they tend to align with each other - and this would be cell adhesion.

Finally, in the model we include concepts that describe the general system, such as cellular temperature which has already been mentioned and means, cellular motility; the tendency of every cell itself to move randomly. Analogously, we include the frequency of reorientations of every cell which when low indicates persistence of movement of a cell in a certain direction.

2.2.2 The rules

Here we discuss how the above assumptions were specifically implemented, and for technical completeness we present the pseudocode for our numerical model in a later section.

First of all, a cell i is an elliptic object with (a_i, b_i) (which we consider integer numbers) its major and minor semi-axes, characterized by

- its position expressed in polar coordinates $\vec{Q}_i = (r_i, \phi_i)$, $r_i \in \mathbb{R}, \phi_i \in \mathbb{R}$,
- its orientation $\theta_i \in [0, \pi]$.

In the previous model, the cells had 4 possible directions of movement with a fixed step size. We would like them to have more freedom in their motion, and for this reason we choose to update their position here in polar coordinates. The algorithm is as follows.

In each time step, cell i counts its neighbours; that is, the number of cells whose center of mass is in a neighborhood $V_i = B(\vec{Q}_i, r_a)$, of center $\vec{Q}_i$, and radius $r_a > 0$ the value of which we specify later. This number is denoted by ρ, and it depends on the choice of r_a.

Similarly, the degree of alignment of every cell with respect to its neighbours is measured in a neighborhood $U_i = B(\vec{Q}_i, r_o)$, where again r_o is a positive number specified later. This measuremengt is achieved by computing first the orientational order parameter S which was defined in Section 1.5, for the cells whose center of mass is in this neighborhood.

The calculation of S

In our case, where $d = 2$, following the formula we mentioned in the previous section, $S = \langle \cos 2\theta \rangle$. In order to compute S, we need first to calculate another quantity called the local director $D(r_o)$, which expresses the average orientation of the cells in U. We do not use the arithmetic mean of the angles, as it would not be adequate; to see this, take for example two cells, one with orientation $\theta_1 = 0$ and another with $\theta_2 = \pi$, for which the arithmetic mean would give us $\frac{\pi}{2}$. However, the cells are in reality parallel, and their real difference is 0 radians. Therefore we use another, more fitting method.

Suppose we have n cells in this area. First, we take the angles $\theta_1, \theta_2, \ldots, \theta_n$ of every cell and we double their value to $\theta' = 2\theta$ Then, we convert $\theta'_1, \theta'_2, \ldots, \theta'_n$ to points on the unit circle, thus in cartesian coordinates $A_1 = (\cos\theta'_1, \sin\theta'_1)$, $A_2 = (\cos\theta'_2, \sin\theta'_2)$, $\ldots$, $(\cos\theta'_n, \sin\theta'_n)$. Then we compute the arithmetic mean of these coordinates, which results in a vector

$$D = (d_1, d_2) = \left(\sum_{i=1}^{n} \frac{1}{n} \cos\theta'_i, \sum_{i=1}^{n} \frac{1}{n} \sin\theta'_i \right),$$

which is the direction vector or nematic director. We then proceed to normalize D (convert it into the unit vector: it is not necessary, but it is done for simplicity), and subsequently for every cell i we calculate the angle Θ_i between the vector defined by its own cartesian coordinates $A_i = (\cos\theta'_i, \sin\theta'_i)$ and vector D. This is equivalent to finding

$$\cos\Theta_i = \frac{A_i \bullet D}{|A_i||D|},$$

where $\bullet$ is the dot product and $|\quad|$ denotes the norm of each vector. Then

$$A_i \bullet D = \cos\theta'_i d_1 + \sin\theta'_i d_2,$$

and

$$|A_i||D| = \sqrt{d_1^2 + d_2^2}.$$

We are finally able to calculate the angle of each cell with the nematic director, which is $\Theta_i' = \arccos(\cos\Theta_i)$.

We proceed to calculate S by averaging over all these angles:

$$S(r_o) = \langle \cos\Theta(r_o) \rangle.$$

In Table 2.1 the pseudocode is presented, in order to provide a clearer picture.

After we have calculated the local density and the local orientational parameter S for all cells, each cell decides whether to move or not as well as whether to rotate. The probability of moving is defined as follows:

$$P_{\text{mov}}(\rho, r_m) = e^{-\lambda_1 \rho(r_m)}.$$

Here, $\lambda_1 > 0$ is a parameter that expresses the cellular temperature of the system. Note that the probability of moving is inversely proportional to the local density.

The probability of rotating is defined as:

$$P_{\text{rot}}(S, r_o) = e^{-\lambda_2 S(r_o)},$$

where $\lambda_2 > 0$ indicates the frequency of reorientations of the cell. It is clear that the more ordered the cells in the neighborhoood are, the less likely it is for the cell itself to rotate.

Two numbers m_1, m_2 uniformly distributed in $[0, 1]$ are generated, and if $m_1 < P_{\text{mov}}$, the cell 'decides' with any direction of movement being equally likely. Thus if (r_t, ϕ_t) are the polar coordinates of the cell at time t, then $x_t = r_t \cos\phi_t$, $y_t = r_t \sin\phi_t$, and

$$\begin{aligned} x_{t+1} &= x_t + \delta r \cos\delta\phi \\ y_{t+1} &= y_t + \delta r \sin\delta\phi \end{aligned}$$

where $\delta r, \delta\phi$ are the step sizes and are uniformly distributed real numbers in $[0, 1]$, $(0, 2\pi]$ respectively.

If $m_2 < P_{\text{rot}}$ the orientation of the cell is also updated with an increment $\delta\theta \in [-1, 1]$.

The basic steps of the algorithm are presented in the form of pseudocode in Table 2.2.

2.2.3 The implementation

For technical completeness, we present here the pseudocode for the calculation of S as well as the basic steps of the algorithm.

Input: List of cells C of length N
Output: S

for all cells i in C **do**
Compute double angle from θ_i
Compute new coordinates for double angle

$$A[i] = (\cos 2\theta_i, \sin 2\theta_i)$$

end for

for all cells i in C **do**
Compute $\Sigma_1 = \sum_i \cos\theta_i$
Compute $\Sigma_2 = \sum_i \sin\theta_i$
end for

Compute director $D = (\frac{\Sigma_1}{N}, \frac{\Sigma_2}{N})$
Compute $|D|$
Normalize $D = \frac{D}{|D|}$

for all cells i in C **do**
Calculate dot product $A_i \bullet D$
Calculate $|A_i||D|$
Compute $\cos\Theta_i = \frac{A_i \bullet D}{|A_i||D|}$
Translate into angle in $[0, \pi]$ $\Theta_i' = \arccos(\cos\Theta_i)$
end for

for all cells i in C **do**
Calculate $S = \sum_i \frac{\cos\Theta_i'}{N}$
end for

Algorithm 2.1: Computation of the orientational order parameter S for a list of cells.

2.2.4 The model as a Markov process

In this Section we discuss the possibility of describing the model as a Markov chain, which is a discrete (but it can also be continuous) time dynamical system that undergoes transitions from one state to another, based on probabilistic rules.

Input: List of cells `allcells` of length M

for all elements i in `allcells` **do**
  Set initial position $\vec{Q}_i$ and orientation θ_i
end for

for step $k = 0, \ldots, L-1$ **do**
  for all elements i in `allcells` **do**
    Calculate number of cells in $V(\vec{Q}_i, r_a)$
    Calculate number of cells in $U(\vec{Q}_i, r_o)$
    Compute local density $\rho(r_a)$
    Compute orientational order parameter $S(r_o)$
  end for
  for all elements i in `allcells` **do**
    Compute P_{mov}
    Compute P_{rot}
    Generate $m_1, m_2 \in [0, 1]$

    if $m_1 < P_{\text{mov}}$ **then**
      Generate step sizes $\delta r \in [0, 1]$, $\delta\phi \in [0, 2\pi]$
      Update position of cell i
    end if

    if $m_2 < P_{\text{rot}}$ **then**
      Generate $\delta\theta \in [-1, 1]$
      Update $\theta_i = \theta_i + \delta\theta$
    end if
  end for
end for

Algorithm 2.2: Basic algorithm for movement and rotation of the cells for L time steps.

Definition. A (discrete-time) Markov chain is a sequence of random variables X_t, $t = 0, 1, \ldots$, that take values on the countable state space $\mathcal{S} = \{i_0, i_1, \ldots\}$, and satisfy the *Markov property*:

$$P(X_t = j | X_0 = i_0, X_1 = i_1, \ldots, X_{t-1} = i_{t-1}) = P(X_t = j | X_{t-1} = i_{t-1}).$$

In other words, the next state of the system depends only on the current state, and the process can be characterized as being memoryless.

Firstly, we would need to define in our framework the states of our system - the state should provide all the information we need to predict adequately the behavior of the system at the next time. Assume that we have just one cell i in the plane with a position $\vec{Q} = (r, \phi)$ and an orientation θ, as defined previously.

Then the state of the cell at a given time t will be the pair $(\vec{Q}, \theta)$. The set S of all possible states of the system, which is the set of all possible pairs $(\vec{Q}, \theta)$ is our state space. Note that in the absence of a lattice, $\mathcal{S}$ is not only infinite, but also uncountable, since r, ϕ and θ all are real numbers.

For the sake of simplicity, we wish to make S easier to define. As a first step, we asssume that the increment δr which is a random number between 1 and 2 has a value fixed to 1. Moreover, the increment $\delta\phi$ which also is generated as a random real number between $[0, 2\pi]$, will be assumed to be an integer between 0 and 360 degrees. Lastly, orientation θ will be assumed to be an integer that ranges between 0 and 180 degrees. as well as the increment $\delta\theta$. In this way, at any given time t cell i has finitely many possible locations that it can obtain and finite number of orientations between 0 and 180 degrees. Therefore, $\mathcal{S}$ becomes now countable.

Now we need to define the transition rates from one state to another.

Suppose we have a cell at a given time t, at a state defined by its position $\vec{Q}$ and its orientation θ. The cell can do one of the following: it can move and rotate simultaneously, can move without rotating, can stay at its position and only rotate, or it can neither move or rotate.

The transition rate of going to a state of new location and new orientation is defined as follows:

$$P_{mov,rot} = P_{mov}P_{rot} = e^{-\lambda_1\rho}e^{-\lambda_2 S}$$

Note that there are $2 * 180$ new locations and $180 - 1$ new *different* orientations, therefore $2 * 180 * 179$ possible new states to which the cell can go with equal probability.

Similarly, the transition rate of moving to a new location and with the same orientation is

$$P_{mov,no-rot} = P_{mov}(1 - P_{rot}) = e^{-\lambda_1\rho}(1 - e^{-\lambda_2 S})$$

The transition rate to a state of the same location but different orientation is

$$P_{no-mov,rot} = (1 - P_{mov})P_{rot} = (1 - e^{-\lambda_1\rho})e^{-\lambda_2 S}$$

Lastly, the transition rate to the last remaining state of staying in the same location without any change in orientation is

$$P_{no-mov,no-rot} = (1 - P_{mov})(1 - P_{rot}) = (1 - e^{-\lambda_1\rho})(1 - e^{-\lambda_2 S})$$

Finally, it is clear from the above that the system described above (for 1 cell) satisfies the Markov property. The probability that a cell i is at a certain state at time t depends only at its previous state (position and orientation). However,

implicitly it depends on the current state of all the other cells in its neighborhood, through ρ and S, which makes it a much more complex process than the Markovian. Moreover, it should also be noted that the state space defined this way is extremely big, which makes it unsuitable for further analysis. The dynamics and properties of the system could be studied in a different framework which will be discussed in Section 4.2.

Chapter 3

Results

In the previous Chapter we discussed two numerical models for the motion of aggregating endothelial cells. The approach presented in Section 2.2 turned out to be the most promising and was analyzed further. In this Chapter we will present the results of simulations performed by implementing this model. It was visualized by using `Gnuplot`, a command-line program that can visualise two- and three- dimensional plots of data.

In the description of the model we always assumed to have elongated cells, of an elliptic shape, which are characterized by their long and short axes (a, b). However, we want also to investigate the effect of cell shape in pattern formation, and for this reason, we distinguish two sets of simulations; in the following section we perform simulations with round cells, whereas in section 3.2 we have cells with a very elongated shape.

3.1 Round cells

Here, the cells are represented as circles with radius 1. In this case they do not rotate, thus their movement is highly dependent solely on the local density as well as the translational parameter λ_1.

We start with 600 cells uniformly distributed across a 400×400 square (thus we have an initial seeding density of $C_1 = \frac{600}{400 \times 400} = 0.00375$), and we keep the translational parameter at a low value $\lambda_1 = 0.5$, which indicates high motility. The radius of interaction for aggregation is $l = 2r = 2$, which indicates that each cell can detect the nearest neighbors in front of and behind it, as well as on its sides. In Figure 3.1, the evolution of the system over 200.000 time steps is shown.

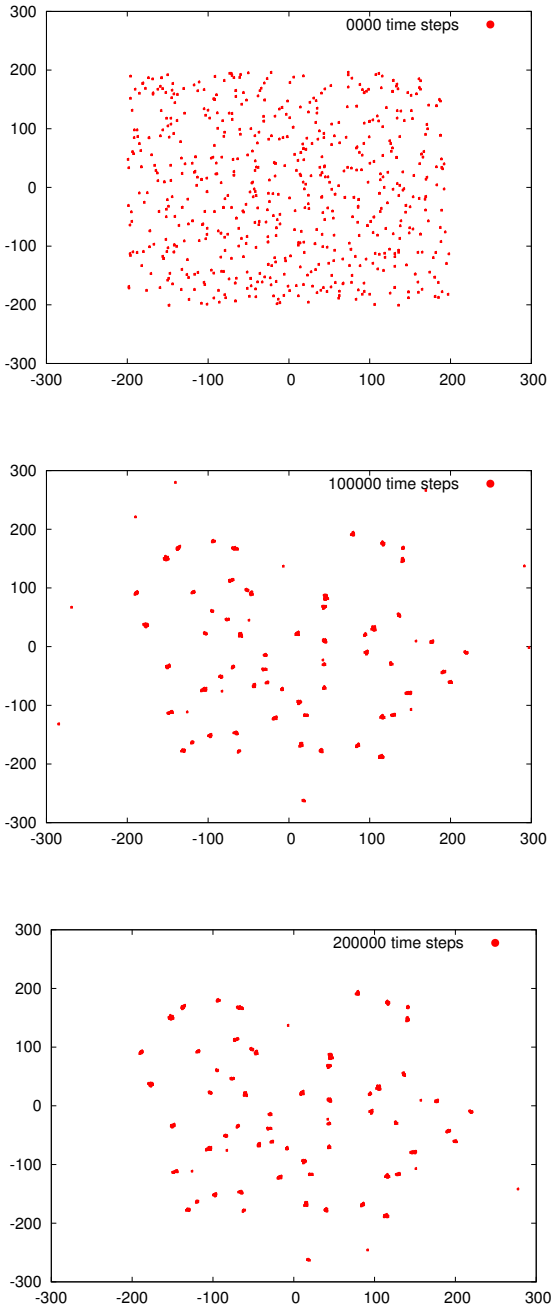

Figure 3.1: Time evolution of round cell movement for $\lambda_1 = 0.5$. across a 400×400 square.

We see that the cells form aggregates, and there are no signs of branch formation or anything network-like. This is something we expected, as it was also observed by means of the simulations of the initial model of Palm and Merks; see first figure of Figure 1.2.

We repeated the simulations with the same parameter values, but with higher

seeding density, as we distribute the cells across a smaller square 200 × 200 (Figure 3.2) and we have $C_2 = \frac{600}{200 \times 200} = 0.015$.

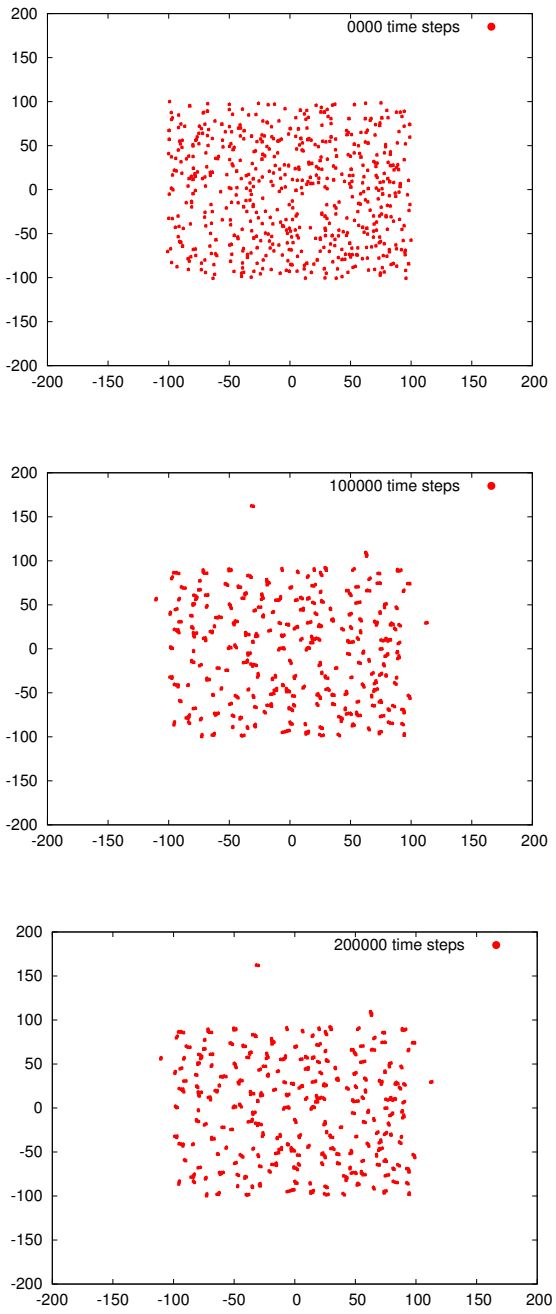

Figure 3.2: Time evolution of round cell movement for $\lambda_1 = 0.5$. across a 400 × 400 square.

We observe that the pattern does not change. We will not investigate further the patterns that arise with the round cells, since this is not the main focus of

this thesis.

3.2 Elongated cells

Change in cell shape gives rise to much more interesting patterns. There is strong interplay among initial seeding density, the rotational and translational parameters λ_1, λ_2 as well as the radii for aggregation r_m and orientation r_o. We observe that as the rotational and translational parameters increase, there is a transition from aggregates to more network-like structures. The radii of interaction for aggregation and orientation have been kept at low values, thus staying close to the nature of the model, where we choose to ignore long range interaction mechanisms.

In our simulations we have 400 cells initially dispersed across a 400×400 square (a density $C_1 = \frac{600}{400 \times 400} = 0.00375$), as with the round cells. They are represented as ellipses; They have however a very elongated shape, resembling thin hard rods, and a length to width ratio **20:1** (where 20 is the length of the long axis, and 1 the length of the short one). They tend to align only with cells that are on their right and on their left, and this is expressed as a radius for orientation $r_o = 10$, which is the length of the major semi-axis a of the elliptic cell. The radius for aggregation is $r_m = 2r = 20$. Figure A.1 in the Appendix shows a morphospace of the patterns for various values of λ_1 and λ_2. A representative sequence can be seen in Figure 3.3.

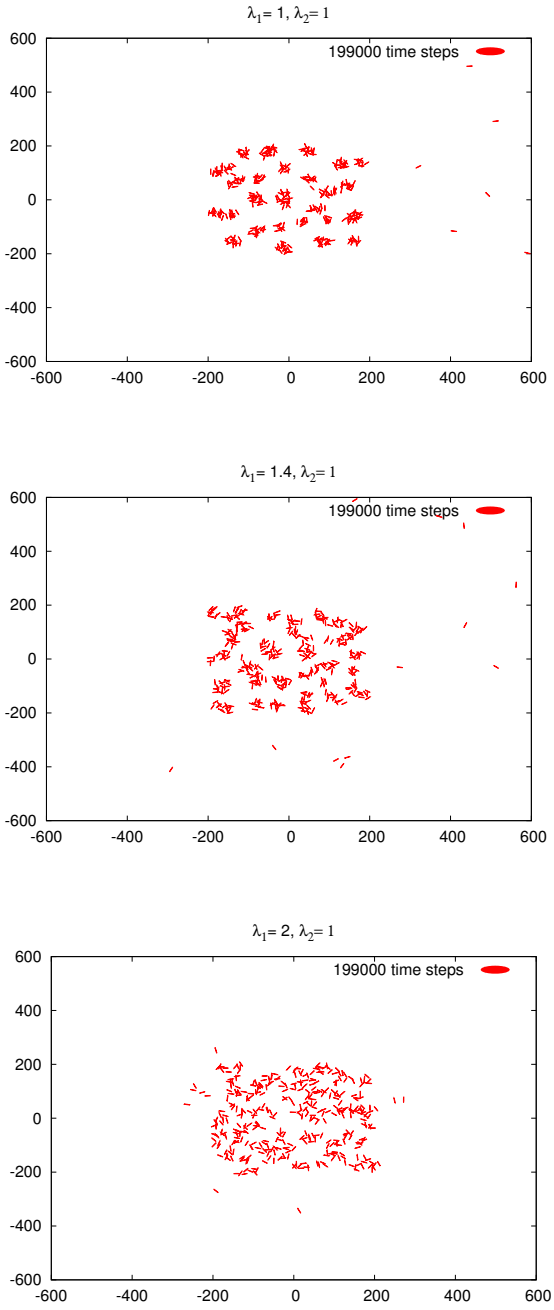

Figure 3.3: Patterns that emerge as the translational parameter λ_1 increases.

As the parameters evolve, the patterns change from being aggregate-like to more stream-like; it seems also that only the moving probability along with λ_1 determine the pattern, and the change in the parameter of the rotation probability doesn't have any effect. It is also clear that there is no long range orientational ordering. This can be confirmed by Figure 3.4, where we see the evolution of the global orientational order parameter over time, for the system with param-

eter values $\lambda_1 = 1.8$ and $\lambda_2 = 5$. Big spikes can be observed, something that indicates continuous changes in the orientations of the cells, and no indication of gradual alignment. It is important to note that we do not expect also S to converge to 1 for a network, but rather remain close to 0.

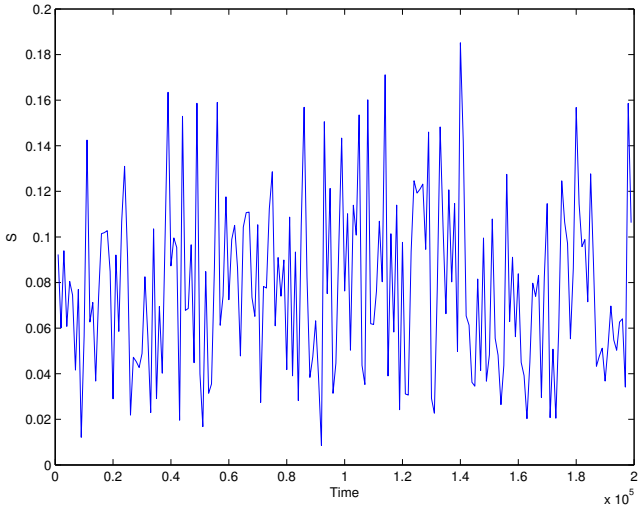

Figure 3.4: Evolution of the global orientational order parameter S for the system with translational parameter $\lambda_1 = 1.8$ and rotational parameter $\lambda_2 = 5$, averaged over 10 simulations.

3.2.1 Persistent movement

Experimental results have shown that elongated cells have bigger directional persistence than rounded cells[20]; this means that their direction of movement is biased tending to be more along their long axis. To incorporate this, we have to slightly modify the equations for the random walk as follows. The position of a cell now is not characterized by (r, ϕ) where ϕ a random angle between $[0, 2\pi]$, but (r, θ), where θ is its orientation. It was easier to express the updates in position in cartesian coordinates. Now, suppose that at time t the position of the cell is $(x_t = r\cos\theta, r\sin\theta)$. At step $t+1$ we update first the orientation $\theta_{t+1} = \theta_t + \delta\theta$, where $\delta\theta$ is uniformly distributed between $[-0.5, 0.5]$ (expressed in radians) and $r_{t+1} = r_t + \delta r$ where δr uniformly distributed in $[0, 1]$ and we have

$$(x_{t+1}, y_{t+1}) = \begin{cases} (x_t + r_{t+1}\cos\theta_{t+1}, y_t + r_{t+1}\sin\theta_{t+1}) & \text{with probability } \frac{1}{2} \\ (x_t - r_{t+1}\cos\theta_{t+1}, y_t - r_{t+1}\sin\theta_{t+1}) & \text{with probability } \frac{1}{2} \end{cases}$$

Note that since θ by definition lies in $[0, \pi]$, we added the possiblity of moving in the opposite direction in the second case.

For our simulations for this variation of the model, we assume that the probability of rotation is low, since persistent motility implies very slow reorientation of the cells and makes a change of its direction less probable.

In our simulations we have 600 cells spread across a 400×400 square, and as before, we kept the radius for aggregation $r = 20$ and for orientation $l = 10$. It is seen also in this case that as the value of the translational parameter λ_1 increases, there is a transition from denser groups of cells to more 'network-like' and 'stream' patterns.The patterns can also be characterized in terms of liquid crystalline ordering; a phase transition can be observed, from (local) nematic order to positional ordering of the cells, which increases as the translational parameter λ_1 becomes higher.

In Figure 3.5 the evolution of the system over time is shown, as the translational parameter λ_1 ranges from 1 to 1.8. The rotational parameter is fixed at a relatively high value $\lambda_2 = 11$. It is good to note that since S is a number always between 0 and 1, the quantity $\lambda_2 S$ is greatly determined by λ_2; nevertheless it never obtains very high values, and therefore there is a good probability of cells rotating.

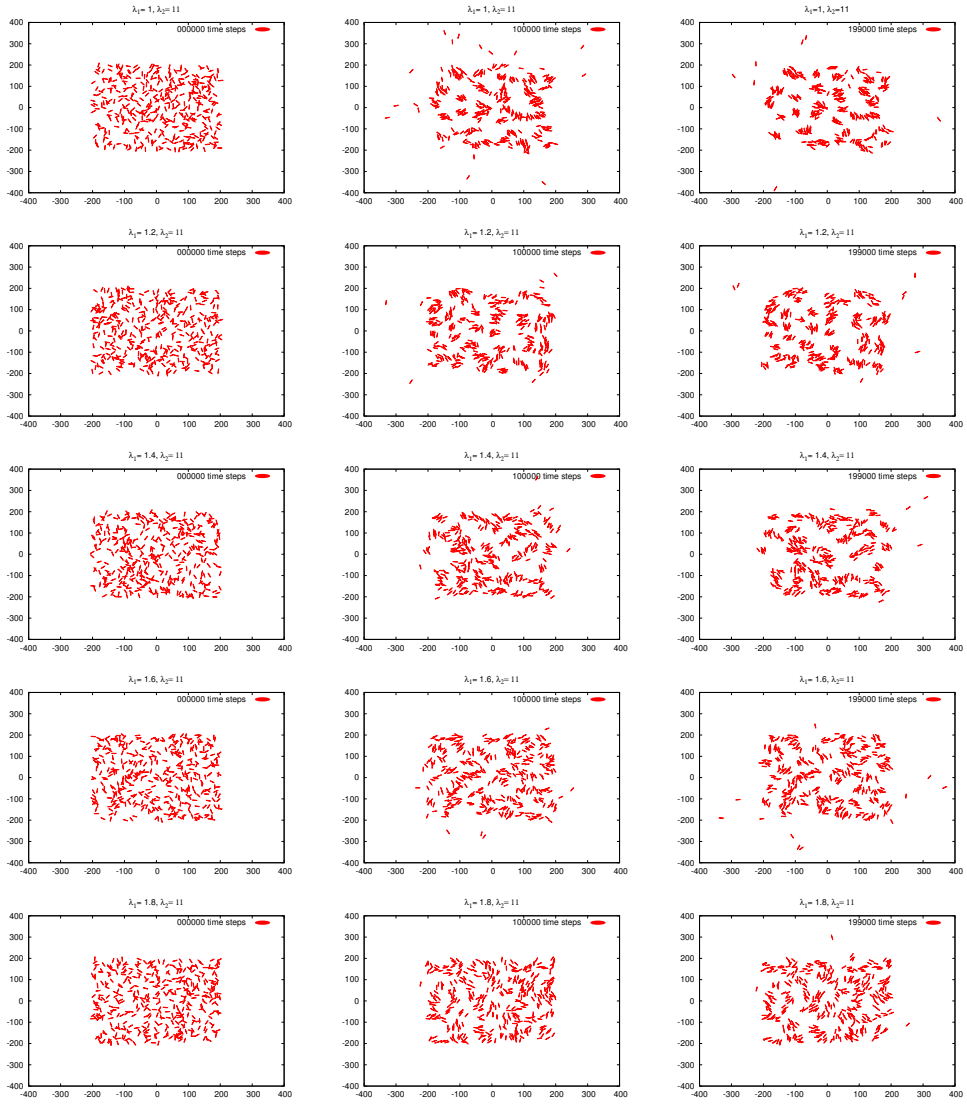

Figure 3.5: Temporal evolution of the system for $\lambda_1 = 1, 1.2, 1.4, 1.8$ and $\lambda_2 = 11$.

The most interesting patterns for us arise in the region 1 - 1.4 for the translational parameter λ_1. Figure 3.10 gives an indicative overview of the different 'states' of the system as the two parameters evolve. For values of $\lambda_1 \leq 0.5$, $\lambda_2 \leq 1.5$, there is no pattern emergence as the system is exhibits a 'liquid-like' phase (not shown in the diagram). As the two parameters increase the phase transition can be seen from aggregating patterns and locally nematic order to a more solid phase since the cells tend to stay still and an increase in the range of this nematic ordering.

We quantified this transition by measuring the cluster size; as a cluster we define the number of cells in a neighborhood of radius $2a$, the centre of which is the position of a cell. It can be seen that the cluster size, or equivalently the density in this area is greater when λ_1 is lower, and decreases when λ_1 becomes higher,

as seen in Figure 3.9.

In a subset of simulations we compressed the cells by spreading them across a smaller square 200 × 200, therefore obtaining a higher density $C_2 = \frac{600}{200 \times 200} = 0.015$, in order to investigate the role of seeding density in pattern formation. It can be seen in Figure 3.6 that there is less aggregation, whereas the alignment process dominates.

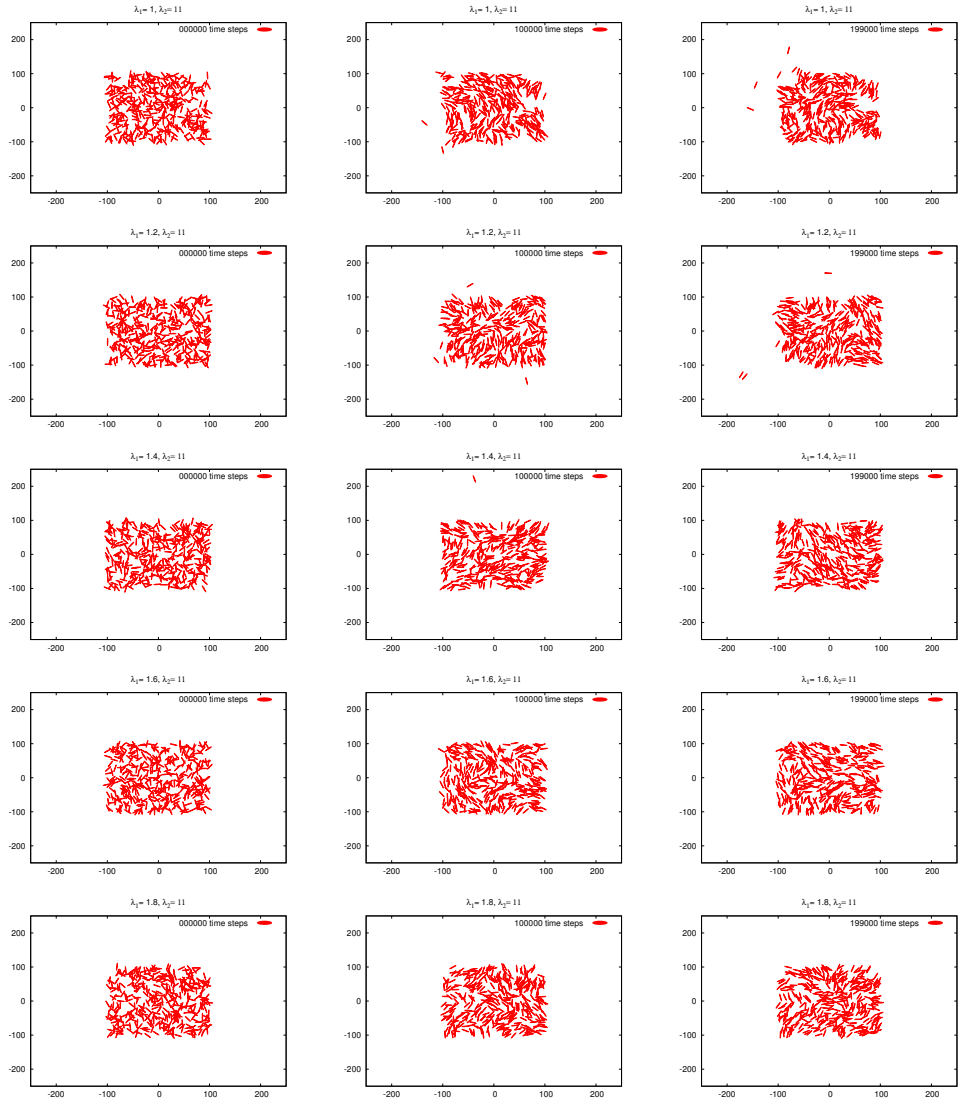

Figure 3.6: Temporal evolution of the system for $\lambda_1 = 1, 1.2, 1.4, 1.8$ and $\lambda_2 = 11$.

In order to illustrate the effect of initial seeding density on the alignment, we compare the evolution of the global orientational order parameters of the two systems, as seen in Figure 3.7.

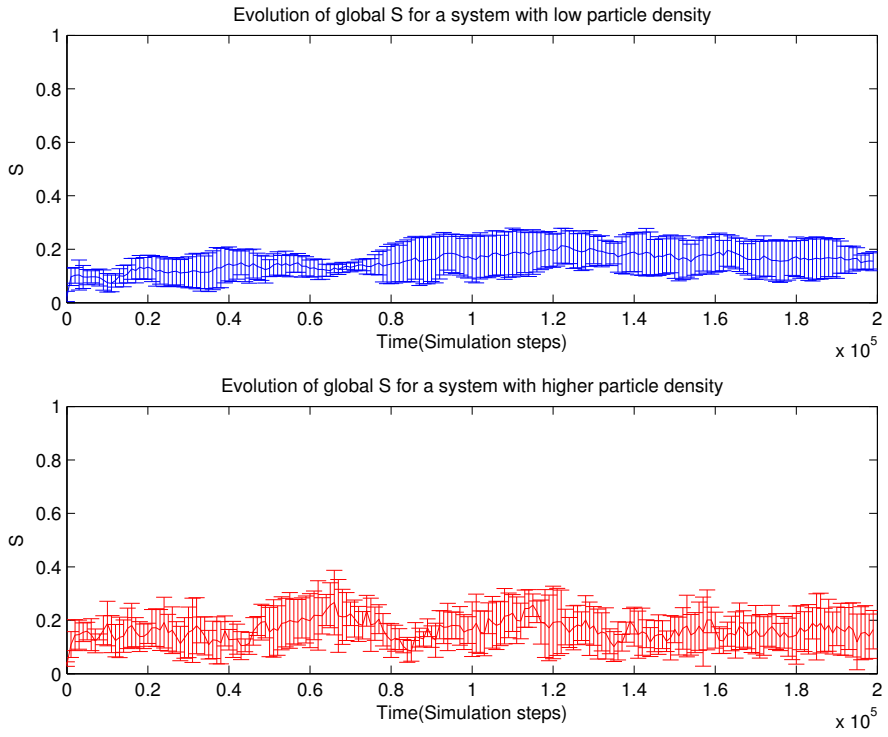

Figure 3.7: Time evolution of global S for the system with the lower density C_1 and S for the system with the higher seeding density C_2.

There is a difference in the global ordering between the two, with more noise in the evolution of S for the system with the densely seeded cells. Nevertheless, in both cases S starts from approximately 0 which indicates un unordered system and remains very low, but increases. This is something that we expect, because it has been already observed in systems where there are aggregating structures or network patterns [13]. S measured globally though is not an adequate quantity, since it could also indicate a system that remains completely unordered. In our case, a more suitable approach would be to measure S locally, and it is expected to be high, which is confirmed below.

As we said, we would like to quantify the degree of local ordering, and how that depends on the radius we use. We studied the temporal evolution of $S(r)$ where $r = 10, 20$ radius around the cells' center of mass, which we present below in Figure 3.8. It is interesting to note that while S globally decreases as seen above, when measured in smaller neighborhoods it is particularly high and very close to 1, something that indicates local ordering. $S(20)$ stays most of the time at values lower than $S(10)$, which is natural, since as $S(r) \to 0$ as r increases.

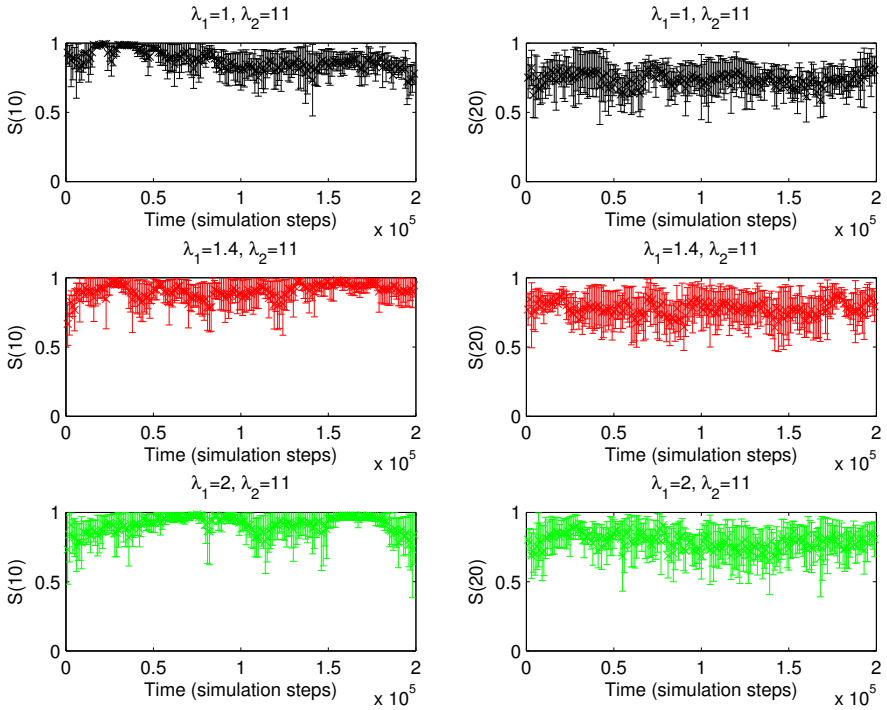

Figure 3.8: Time evolution of $S(10)$, $S(20)$, averaged over 10 simulations.

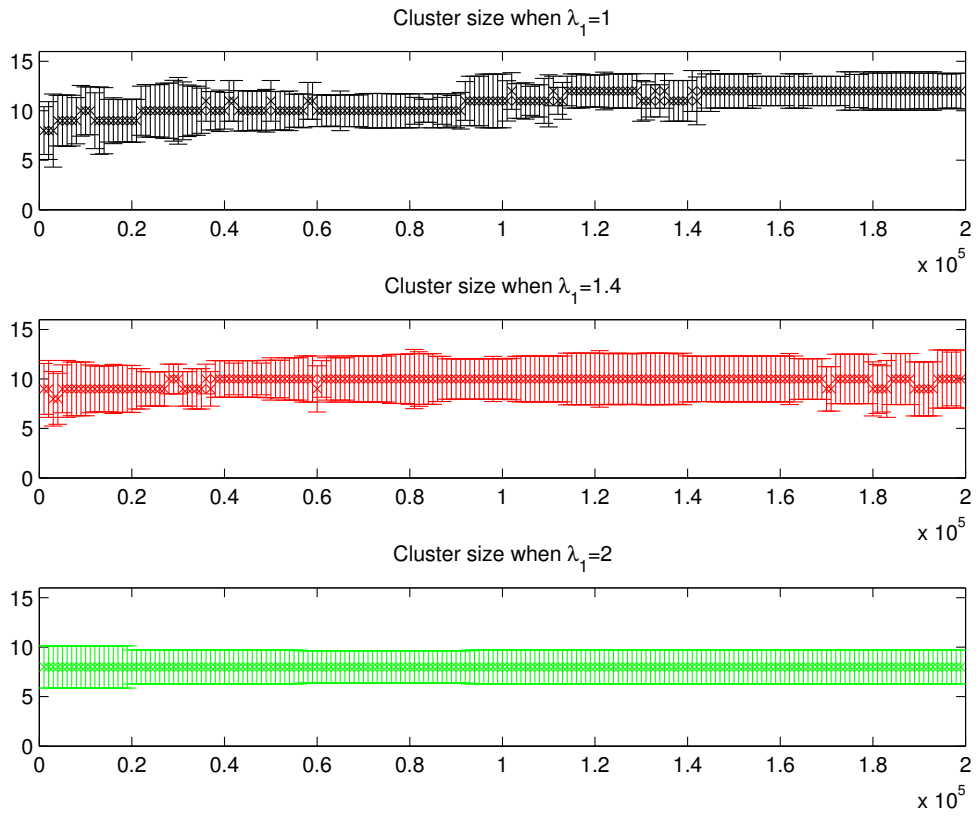

Figure 3.9: Cluster size for $\lambda_1 = 1, 1.4, 2$, $\lambda_2 = 11$ averaged over 20 simulations with SD error bars. Vertical axis: number of cells in a neighborhood. Horizontal axis: time in simulation steps.

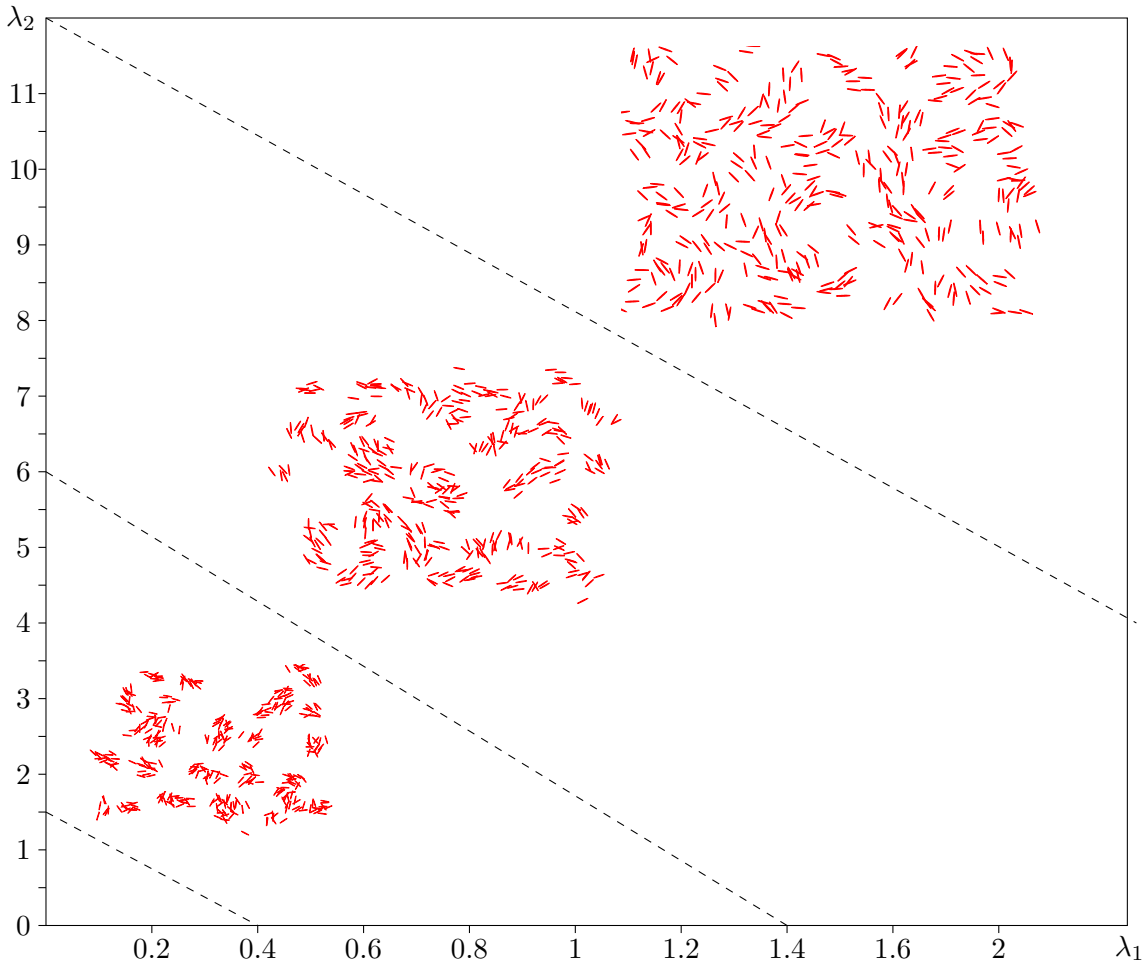

Figure 3.10: Indicative phase diagram of the system for λ_1, λ_2.

3.2.2 Radii for aggregation and orientation

As was mentioned before, we would like to avoid in general increasing the radii for aggregation and orientation, since that would imply existence of long range interaction among the cells. However, we did run some experiments where we slightly increased the radius of aggregation, and kept the rest of the parameters the same. This resulted in very low cellular motility and no emergence of interesting patterns.

3.3 Summary

The results of our simulations confirm the observations made with the computational Cellular Potts model; it is seen that elongated shape combined with movement towards a preferred direction play an important role in the formation of network-like structures. It is shown that local alignment is much higher than the global one, which is in agreement with what was observed in the simulations with the Cellular Potts; the cells in both cases tend to align locally with their adjacent cells. In our simulations there is gradual organization of cells into groups the size of which tends to stabilize as time passes since the cells tend to remain still. However, the cells do move and rotate always with a very small probability tending to align, therefore it cannot be said that the system has reached a steady state; this is very close to the arrested dynamics pattern as seen in the original model.

Chapter 4

Further analysis

In the previous chapters, we proposed and discussed a numerical model, which we hoped would be able to give more insight into the phenomenon of arrested dynamics, as seen in the simulations of the computational model described in Section 1.2.2. We attempted to reduce many complex details that regard biophysical cell properties and cell interactions as implemented in the Cellular Potts model to a rather simple set of rules. These rules allowed us to study the collective effects on cell motion due to their local interactions.

The results obtained with the simulations are in qualitative agreement with those of the simulations with the Cellular Potts; we were able to reproduce quite accurately the evolution of the global as well as the local ordering. In both models the behavior of the orientational order parameters is the same. Moreover, we were able to reproduce the gradual creation of clusters and the slow evolution of the system to an arrested dynamics, non-equilibrium state; in our case, from a certain point onwards cells tend to remain still and rotate much less. Nonetheless, some still move and rotate with a very small probability, tending to align, something that implies that the system has not reached its final steady state.

Therefore, it can be said that the primary goal of this work is achieved: reproduce the behavior observed with the Cellular Potts, by using a simpler numerical model which would be suitable for further analysis. The model we presented is able to reproduce the desired behavior including all the initial biological assumptions; its strengths compared to the Cellular Potts are that every cell can be considered as one particle (with dimensions) to which all properties are assigned; secondly, diffusion and rotation are independent, which makes it possible to examine better their effect separately on the collective behavior. Now, we would like to go a step further and propose two possible approaches for further analysis.

4.1 Diffusion-limited aggregation

In this section we discuss a different, and broad mathematical framework in which the phenomenon of aggregating particles is studied. It is of interest to us because its phenomenology and certain elements share similarities with our model, as was seen in the previous chapters.

The initial DLA is a model proposed by Witten and Sander in 1981[21], which describes formation of aggregates by diffusing and self-organising particles. Phenomena that can be described by the previous sentence occur in many different systems in physics, chemistry and biology, such as electrodeposition, growth of bacteria colonies, or dielectric breakdown. The DLA model manages to describe such irreversible growth phenomena while being relatively easy to formulate and implement.

The basic algorithm itself is very simple. Initially, there is one particle (which we will call *seed*) fixed in space, usually placed in the center of a circle of an arbitrary radius. Then another particle is released, relatively far from the circle, and starts undergoing a random walk. It continues until it meets the seed, in which case it stops, or until it goes too far away from the circle (surpasses a certain 'elimination distance') in which case it is discarded. Once its route has ended, another random walker is released, which undergoes the same procedure until it meets the previous particles or it is discarded, and so forth. The particle probability distribution is governed by the Laplace equation. Note that the density of the particles has to be low, so that only the diffusive nature of the system is present. This iterative stochastic process is able to produce interesting asymptotic behaviour, and leads to formation of structures with complex geometry. The clusters that are formed are typical examples of a fractal - see Figure 4.1. This is the most important characteristic of the DLA; systematic and analytic calculation of the size and exploration of the geometrical and statistical properties of these aggregates is one of the main goals. This comes down to calculating a number called the fractal dimension of the clusters, and indicates how the fractal structure scales differently from the space in which it is embedded; often, the scaling dimension is not an integer.

Naturally, in one dimension the problem is very easy, as every cluster is a line segment, and every time a particle is added randomly to one or the other side. In three dimensions, it has been shown that several methods employed to calculate cluster size work well.[22].

In two dimensions, however, the problem becomes more complicated, as these interfacial structures emerge, which are too complex to be characterized as 1-dimensional, but too simple to be 2-dimensional. Due to its simplicity when it comes to the implementation, DLA in two dimensions has been studied mostly be means of computer simulations.

The phenomenology of our model presents similarities with the DLA models. In both models the main element is translational and rotational diffusion of the

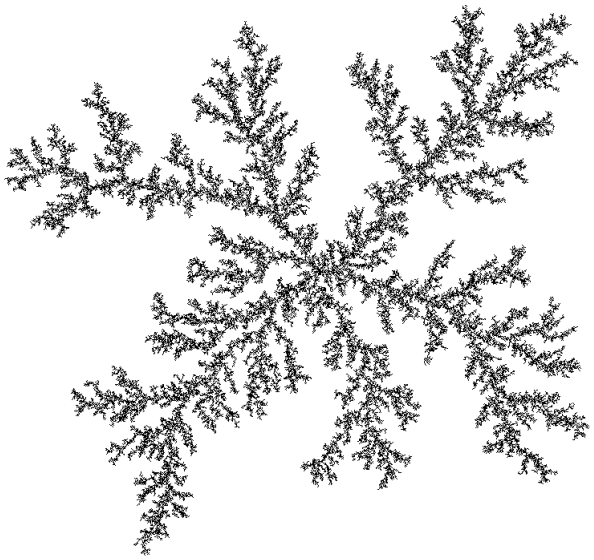

Figure 4.1: Example of a fractal structure with diffusion-limited aggregation (Image courtesy of P. Bourke, www.paulbourke.net).

particles, which results in formation of aggregates. After these aggregates are formed, the cells remain still. Our model differs phenomenologically though in two points: firstly, there is no restriction when it comes to deattachment of the particles; however, it is highly unlikely, therefore it can be considered as an almost irreversible phenomenon. Secondly, the random walkers are released simultaneously and not one after the other as in the original DLA, therefore a different approach for multiple particles should be followed. A variant for multiparticle DLA was discussed by Sanchez et al [23], where a finite number of random walkers is released simultaneously instead of one, and Castro et al. [24], where particles choose one of their neighbors as destination sites and attach to them with a certain 'sticking' probability.

The difficulty of the DLA lies in its non-equlibrium nature, therefore it is not related to a class of problems in equilibrium statistical mechanics for which analytical methods have been proposed. Nonetheless, in our opinion, a characterization of the structures in terms of their fractal dimension would be interesting and suitable; something similar was done for colloidal particles [25] which diffuse anisotropically in a viscous fluid; a behavior similar to the one we presented. The effect of the particle shape on the size of the cluster was explored, with the authors determining that also in the case of quasi 1-dimensional hard rods.

4.2 Interacting particle systems

Rigorous mathematical analysis could give us more insight into the long-time behavior of the system. From the attempt we made to describe the model

as a Markov chain it becomes clear that the choice of the state space as well as the transition rates is crucial; there is of course no 'right' choice: different formulations lead to different approaches and tools.

The area of interacting particle systems, developed and studied intensively in the last twenty years, can provide such tools. The field is now a quite large branch of probability theory and measure theoretic probability, of which we will hardly attempt to scratch the surface.

The whole field is concerned with systems of (infinitely many) interacting components. Quite generally, one considers agents or particles located at the sites of a lattice. Each site is assigned a state, the change of which is dependent on the states of the other sites. The interactions are considered strictly local, in the sense that only one or two sites change state at a given time, and moreover there is no long range interaction; in most cases, the change of a state depends on the states of the neighboring sites. The systems are modelled as continuous time Markov processes, and the questions that are investigated regard the nature of the stationary states and the existence of such stationary distributions.

Below, we give briefly some formal definitions. We have used as our frame of reference literature by Liggett [26].

4.2.1 General setup

Suppose that we have a countable set of sites S (usually $\mathbb{Z}^d$), and K is a finite set of possible states at a site. Then K^S is the set of the configurations of a system and will be the state space for the models we consider. A configuration is the set of variables that characterizes what the system is doing at a given time - in our case, all the states of the system at a given time.

An *Interacting Particle System* is a Markov process $\eta = (\eta_t)_{t\geq 0}$ on the state space $\Omega = \{0,1\}^{\mathbb{Z}^d}$, $d \geq 1$. We denote as $\eta_t(x)$ the state at site x at a given time t.

One can interpret the states in different ways. When $\eta_t(x) = 1$ or 0 it can mean that there is a particle or a 'hole' at site x at time t, respectively; in another case, 1 means an infected individual and 0 a healthy one, etc. The evolution is determined by specifying a set of local transition rates

$$c(x, \eta)$$

expressing the rates of change when the system is in configuration η, when the state at x changes. Therefore saying that the transition occurs at rate c means that

$$P^{\eta}(\eta_t(x) \neq \eta) = c(x, \eta)t + o(t), \qquad t \to 0.$$

In the systems we discuss there are only two possible states at each site, and

such systems are called *spin-flip* systems; however, it is certainly possible to have more than two states. Moreover, the interactions are considered strictly local, in the sense that only one or two sites change states at a given time, and the rates of such transitions depend on the states of the nearby sites.

The exact relation of the process and its transition rates is described by its infinitesimal generator Ω. It is a typically unbounded operator defined on an appropriate dense subset of $C(\{0,1\}^S)$, and it is determined by its values on the cylinder functions, i.e. functions that depend on finitely many coordinates. In that case it takes the form

$$\Omega f(\eta) = \sum_{\zeta} c(\eta, \zeta)[f(\zeta) - f(\eta)],$$

where $c(\eta, \zeta)$ are the transition rates from η to ζ. The rates that we will choose for our models will have to be such that the above series converges uniformly for cylinder functions f.

We will now present and discuss examples of these systems. We will need first though to introduce the following notation: if $\eta \in \{0,1\}^S$ and $x, y \in S$, then $\eta_x, \eta_{x,y} \in \{0,1\}^S$ are defined by

$$\eta_x(u) = \begin{cases} \eta(u) & \text{if } u \neq x \\ 1 - \eta(u) & \text{if } u = x \end{cases}$$

and

$$\eta_{x,y}(u) = \begin{cases} \eta(u) & \text{if } u \neq x, y \\ \eta(y) & \text{if } u = x \\ \eta(x) & \text{if } u = y \end{cases}.$$

This means in practice that η_x is obtained from η by changing its value at x, and $\eta_{x,y}$ is obtained by interchanging the values of x and y. The second case (the transition of $\eta \to \eta_{x,y}$) can be seen as the movement of a particle from x to y, or from y to x.

An example of an interacting particle system, which also has been a starting point for the development of this theory, is a model of magnetization.

4.2.2 The stochastic Ising model

The stochastic Ising model is taken from the field of statistical mechanics, and it was one of the first models of this type to raise interest in the field. Take $S = \mathbb{Z}^d$, the d-dimensional integer lattice (which represents the sets of iron atoms) and $K = \{-1, +1\}^{\mathbb{Z}^d}$ the state space - the possible spins of an atom. Let $\beta > 0$

express the temperature, and suppose that the rate at which the spin at site $x \in \mathbb{Z}^d$ flips is

$$c(x, \eta) = e^{-\beta\eta(x)\sum_{y\sim x}\eta(y)},$$

where $y \sim x$: all y such that$|y - x| = 1$ (y are the neighboring sites of x). Note that the flip rate is relatively large when the spin of x is different from the spins of most of its neighbors, while it is smaller if the spins are the same. This means that spins prefer to align with the majority of the neighboring spins.

The next kind of interacting particle system we will present is the one of most interest to us; its dynamics resemble strongly those of the model we proposed.

4.2.3 The exclusion process

These processes are different from the ones described above, and are most relevant for our problem; the reason is that they allow transitions to change values at two sites at a time rather than only one. This makes them suitable for modelling particle motion or traffic flow; the first use of this model though was in a biological context, for the modelling of ribosomes.

Again, S is a countable set, and $p(x, y)$ are the transition probabilities for a Markov chain on S. We must also assume that

$$\sup_y \sum_x p(x, y) < \infty$$

in order to ensure that the generator as seen below is well defined. The transition rates for this process are determined as follows:

$$\eta \to \eta_{x,y} \text{ with probability } p(x, y) \text{ if } \eta(x) = 1, \eta(y) = 0.$$

In this setting, the states 0 and 1 represent sites that are either empty (0) or occupied by a particle (1), and there is at most one particle per site. A particle at x waits a unit exponential time T (one for which $(P(T > t) = e^{-t})$ and then chooses a site y to which it tries to move with rate $p(y, x)$. If y is vacant, it moves to that site, while if it is occupied, the change in position is suppressed, thus the 'exclusion' term.

The generator for this process is of the form

$$\Omega f(\eta) = \sum_{\eta(x)=1,\eta(y)=0} p(x, y)[f(\eta_{x,y}) - f(\eta)],$$

where f are the cylinder functions. Note that for the above series to converge uniformly and thus define a continuous function on $\{0, 1\}^S$, the assumption made previously on the sum of the transition rates is necessary.

The goal then is to determine the nature of the class I of stationary distributions for this process, and if possible to determine them explicitly, which has been achieved, by using techniques such as coupling and duality for stochastic processes. The nature of the stationary distributions depends on whether the process is symmetric (i.e. $p(x,y) = p(y,x) = \frac{1}{2}$) or not. It is proved that the long term behavior of the process is more complex in the absence of symmetry.

4.2.4 Our model as an exclusion process

We believe that the field of interacting particle systems and in particular the exclusion process provide a rigorous mathematical framework which could give more insight into the dynamics of the model we proposed. The model can be considered a system with finitely many components which interact locally via adhesion as described in the previous chapters. The analysis of the model in the framework of exclusion processes is the most suitable one in our opinion: it is a process used primarily in order to describe particle motion. Moreover, as described above, the main element of the exclusion process is its strong repulsion dynamics, which prevent occupation of a site by more than one particle. This is an element that is very much present in our model as well, although it is a bit less strict; theoretically, occupation of one site by more than one particle is possible, but the probability of this event is very low.

Two issues arise with the modelling of the system as an exclusion process. First of all, the model we proposed is off-lattice, unlike all interacting particle systems. Secondly, in our model we have elongated objects which are characterized by their orientation. Adding this property to the particles in the framework of IPS would make the process much more complex; however, the idea behind these systems is to see what are the major elements that alone can give rise to the required phenomena, without taking into account every detail. The strength of these systems is the simplicity and shortness of the rules, and the possible richness of the behavior that arises from them. One could argue that taking into account the dimensions of our cells in order to investigate the nature of their motion in long term is not necessary; note that when we define the rules for their movement we do not take into account their dimensions, but consider only their center of mass.

Therefore, we will attempt to formulate the model as follows.

Consider a two dimensional square lattice. Each site $\bar{x} = (x, y)$ takes a value $\eta(x)$ from the state space $\Omega = \{0, 1\}$, which is 0 if the site is empty or 1 if the site is occupied by a cell. Each cell in site $\bar{x}$ waits an exponential waiting time and then chooses one of the four adjacent sites with equal probability (it cannot move to a diagonal direction). It attempts to move to the chosen site $\bar{x'}$ with a probability that depends on the number of the vacant (occupied) adjacent sites. This is the transition probability from state $\eta(\bar{x}) = 1$ to $\eta'(\bar{x}) = 0$ for site $\bar{x}$. Using the notation from the previous section, we can define the transition rate as follows:

$$c(\bar{x}, \eta) = e^{-\lambda_1 \sum_{\bar{y} \sim \bar{x}} \eta(\bar{y})},$$

where $\bar{y} \sim \bar{x}$ describes all adjacent sites $\bar{y}$ to $\bar{x}$, and λ_1 is the translational parameter (see Section 2.2) defined in the previous chapters.

Moreover, we consider the exclusion process with open boundaries. We assume that at the borders of the lattice, a particle can leave the lattice with rate α which is site-independent, and a particle can be added to the site (if vacant) with rate β.

The Markovian dynamics can be seen also in terms of networks (graphs), where the states of the stochastic process correspond to the nodes (vertices) of the network. Each transition allowed by the dynamics represents an edge, and the corresponding rate is the weight for that edge. Any state can be reached by any site on the network, which means that the network is connected.

Another approach that could be taken is the following. It is based on a model for cell-cell adhesion introduced by Khain et al. in [27]. Consider i and j two lattice sites. Then denote by $M(i, j)$ the set of lattice sites that are nearest neighbors (adjacent) both to i and j, and $m(i, j)$ the number of occupied sites between them. Moreover, denote by $N(i, j)$ the set of lattice sites that that are the nearest neighbors of i but not of j, and then $n(i, j)$ the number of occupied sites between them. Then, the authors defined the transition rate of a particle from site i to site j as

$$T_{i,j} = (1 - q)^{m(i,j)+n(i,j)}.$$

$q \in [0, 1]$ being a constant parameter to quantify the strength of adhesion. If $q = 0$, there is no adhesion and the particle moves to site j with rate 1, whereas movement becomes impossible when $q = 1$ in the case of strong adhesion resulting in the particle remaining still.

The first definition of the transition rates would be more appropriate, since it stays closer to the numerical model that is proposed.

Chapter 5

Discussion

5.1 Conclusions and future work

We presented and implemented a simple, off-lattice model in order to describe the motion of aggregating endothelial cells. By using a more stochastic approach, which stays close to the nature of the initial model, our purpose was to examine whether self-organization of adhesive cells is sufficient for formation of vascular-like patterns. We started with particles to which we added dimensions, making them rounded or elongated, as well as orientation. We formulated simple rules that govern their movement and orientation, with which we were able to reproduce network-like structures, in the absence of any long range interaction mechanisms. Factors such as persistent motility, rotational diffusion rate and 'cellular temperature' were incorporated in the model and expressed by the two main parameters λ_1 and λ_2.

The results of our simulations are in qualitative agreement with experimental as well as theoretical observations; it is shown that cell shape combined with directional persistence have an important effect on vascular network formation. Using terminology from the theory of liquid crystals, we determined and quantified by using orientational order parameters a transition from local nematic ordergin to a more solid phase. There are also similarities with 'wood grain' patterns studied by E. Kramer [28]. We were able to reproduce the behavior of the Cellular Potts model of angiogenesis, something that was validated by looking at the evolution of the orientational order parameters as well as the gradual formation of clusters. It was also observed that the system always evolves since the cells continuously rotate and move with gradually smaller probability - a pattern equivalent to the arrested dynamics of the first model.

We believe that the model proposed is a good first step towards further analysis, since it is an agent-based model which includes many of the biological assumptions that we wanted to test and by construction is easy to analyse - the numerous constraints of the Cellular Potts are absent. We considered the possibility of studying it within the diffusion limited aggregation framework; however, despite

the similarities between the two models, there are difficulties in the analytical tractability and therefore, an alternative approach was considered.

By the way the model is constructed, it allows us to study it in a rigorous mathematical framework such as the interacting particle systems, and in particular the exclusion process, a model that has been studied extensively. Therefore, the important next step - the study of the long term behavior of the model with an analytical approach, is certainly possible. It would require further semplification with the representation of the cells as particles on a lattice, and an appropriate modification of the transition rates, but it has the possiblity to yield the most interesting theoretical results.

Appendix A

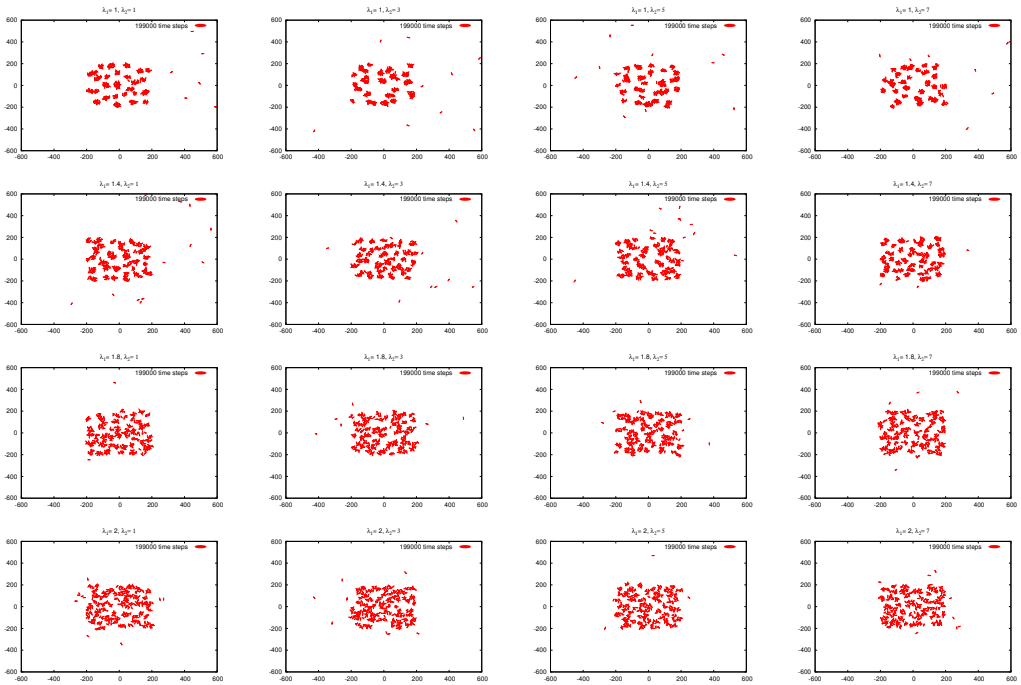

Figure A.1: Morphospace of the system when $\lambda_1 = 1, 1.4, 1.8, 2$ and $\lambda_2 = 1, 3, 5, 7$.

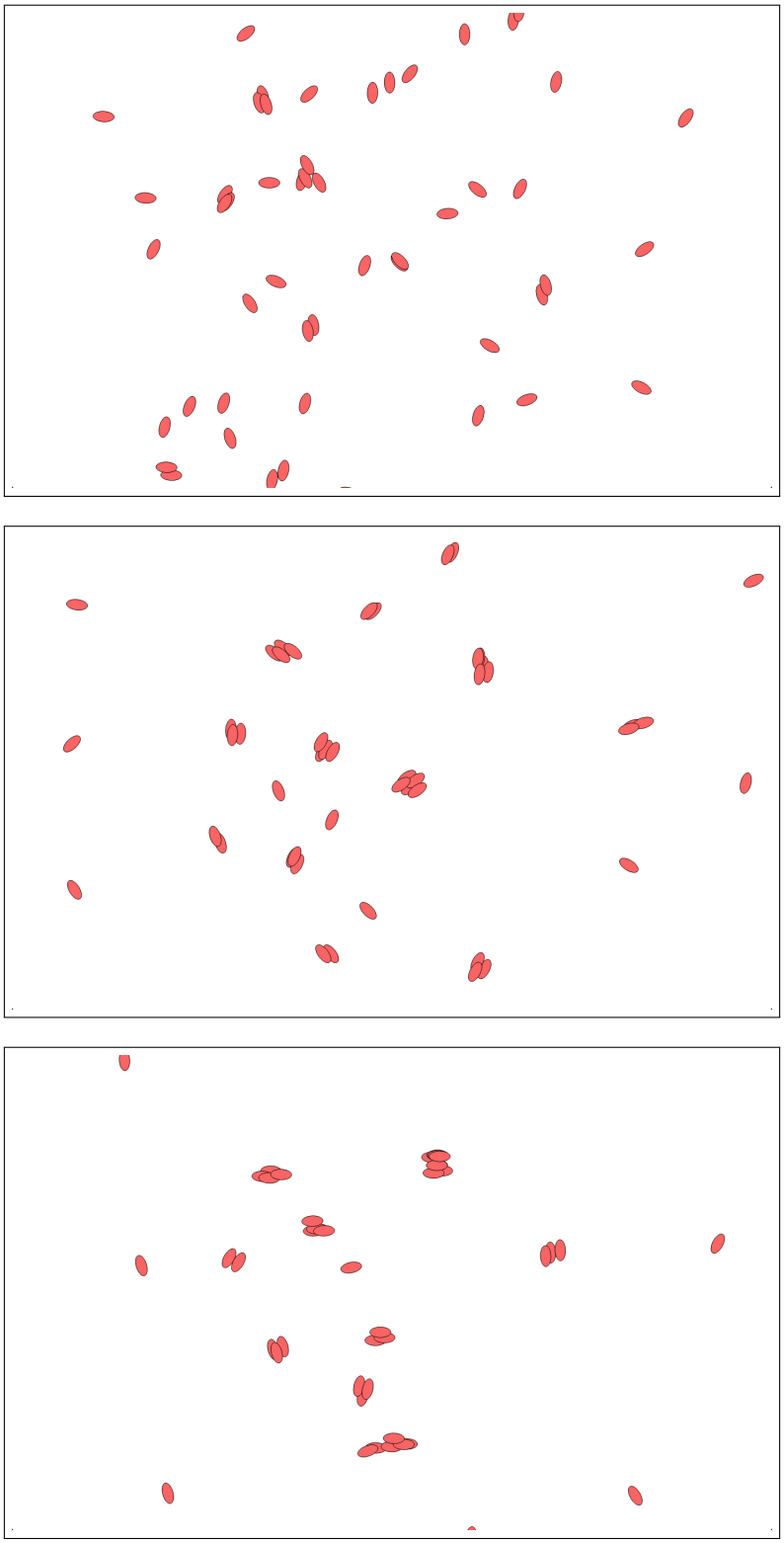

Figure A.2: Temporal evolution of a system of 70 cells using the Qt library.

Bibliography

[1] Werner Risau. "Mechanisms of angiogenesis". In: *Nature* 386.6626 (1997), pp. 671–674.

[2] J Folkman and Y Shing. "Angiogenesis." In: *Journal of Biological Chemistry* 267.16 (1992), pp. 10931–10934. eprint: `http://www.jbc.org/content/267/16/10931.full.pdf+html`. URL: `http://www.jbc.org/content/267/16/10931.short`.

[3] Judah Folkman. "What is the evidence that tumors are angiogenesis dependent?" In: *Journal of the National Cancer Institute* 82.1 (1990), pp. 4–7.

[4] Judah Folkman. "Tumor angiogenesis". In: *Adv Cancer Res* 43.1 (1985), p. 174.

[5] Tamás Vicsek et al. "Novel type of phase transition in a system of self-driven particles". In: *Physical Review Letters* 75.6 (1995), p. 1226.

[6] Guillaume Grégoire, Hugues Chaté, and Yuhai Tu. "Moving and staying together without a leader". In: *Physica D: Nonlinear Phenomena* 181.3 (2003), pp. 157–170.

[7] D Manoussaki et al. "A mechanical model for the formation of vascular networks in vitro". In: *Acta Biotheoretica* 44.3-4 (1996), pp. 271–282.

[8] Guido Serini et al. "Modeling the early stages of vascular network assembly". In: *The EMBO Journal* 22.8 (2003), pp. 1771–1779.

[9] D Ambrosi, A Gamba, and G Serini. "Cell directional and chemotaxis in vascular morphogenesis". In: *Bulletin of Mathematical Biology* 66.6 (2004), pp. 1851–1873.

[10] François Graner and James A Glazier. "Simulation of biological cell sorting using a two-dimensional extended Potts model". In: *Physical review letters* 69.13 (1992), p. 2013.

[11] Roeland MH Merks et al. "Contact-inhibited chemotaxis in de novo and sprouting blood-vessel growth". In: *PLoS computational biology* 4.9 (2008), e1000163.

[12] Roeland MH Merks et al. "Cell elongation is key to in silico replication of in vitro vasculogenesis and subsequent remodeling". In: *Developmental biology* 289.1 (2006), pp. 44–54.

[13] Margriet M Palm and Roeland MH Merks. “Vascular networks due to dynamically arrested crystalline ordering of elongated cells”. In: *Physical Review E* 87.1 (2013), p. 012725.

[14] Rhoda J Hawkins, Simon H Tindemans, and Bela M Mulder. “Model for the orientational ordering of the plant microtubule cortical array”. In: *Physical Review E* 82.1 (2010), p. 011911.

[15] Simon H Tindemans, Rhoda J Hawkins, and Bela M Mulder. “Survival of the aligned: ordering of the plant cortical microtubule array”. In: *Physical review letters* 104.5 (2010), p. 058103.

[16] Angela Stevens and Hans G Othmer. “Aggregation, blowup, and collapse: The ABC’s of taxis in reinforced random walks”. In: *SIAM Journal on Applied Mathematics* 57.4 (1997), pp. 1044–1081.

[17] R. Eppenga and D. Frenkel. “Monte Carlo study of the isotropic and nematic phases of infinitely thin hard platelets”. In: *Molecular Physics* 52.6 (1984), pp. 1303–1334. DOI: 10.1080/00268978400101951. eprint: http://www.tandfonline.com/doi/pdf/10.1080/00268978400101951. URL: http://www.tandfonline.com/doi/abs/10.1080/00268978400101951.

[18] Anna A Mercurieva and Tatyana M Birshtein. “Liquid-crystalline ordering in two-dimensional systems with discrete symmetry”. In: *Macromolecular Theory and Simulations* 1.4 (1992), pp. 205–214.

[19] Christopher Harrison et al. “Dynamics of pattern coarsening in a two-dimensional smectic system”. In: *Physical review E* 66.1 (2002), p. 011706.

[20] S Huang et al. “Symmetry-breaking in mammalian cell cohort migration during tissue pattern formation: Role of random-walk persistence”. In: *Cell motility and the cytoskeleton* 61.4 (2005), pp. 201–213.

[21] TA Witten Jr and Leonard M Sander. “Diffusion-limited aggregation, a kinetic critical phenomenon”. In: *Physical review letters* 47.19 (1981), p. 1400.

[22] M Tokuyama and K Kawasaki. “Fractal dimensions for diffusion-limited aggregation”. In: *Physics Letters A* 100.7 (1984), pp. 337–340.

[23] Angel Sánchez, MJ Bernal, and JM Riveiro. “Multiparticle aggregation model for dendritic growth applied to experiments on amorphous Co-P alloys”. In: *Physical Review E* 50.4 (1994), R2427.

[24] Mario Castro et al. “Multiparticle biased diffusion-limited aggregation with surface diffusion: A comprehensive model of electrodeposition”. In: *Physical Review E* 62.1 (2000), p. 161.

[25] Jacob R Rothenbuhler et al. “Mesoscale structure of diffusion-limited aggregates of colloidal rods and disks”. In: *Soft Matter* 5.19 (2009), pp. 3639–3645.

[26] Thomas M Liggett. *Interacting particle systems*. Springer, 2005.

[27] Evgeniy Khain, Leonard M Sander, and Casey M Schneider-Mizell. “The role of cell-cell adhesion in wound healing”. In: *Journal of Statistical Physics* 128.1-2 (2007), pp. 209–218.

[28] Eric M Kramer. “A mathematical model of pattern formation in the vascular cambium of trees”. In: *Journal of Theoretical Biology* 216.2 (2002), pp. 147–158.